II. Performance of Filter Media in Liquid Service

The performance of nine typical filter media of previously determined pore structure has been determined by the filtration of very dilute suspensions containing spherical particles of known size distribution. The mechanisms of filtration prior to the formation of a macroscopic cake are considered, and the applicability of various filtration laws proposed by Hermans and Bredée to describe these regions of filtration are examined. Regions of "standard-blocking" filtration are found to occur with each of the filter media examined. The clogging values for the various media over the region of standard blocking are shown to be related quantitatively to the modal value of interfiber pore radius of the media, as measured by the mercury-intrusion method.

Part I of this paper examined the internal structure of typical filter media commonly used for liquid filtration and presented data on the pore size and pore-size distribution of these media. In this second part the performance of these same filter media is determined quantitatively by a clarification technique, and the clogging values for the various media are correlated with the previously reported pore-size-distribution data.

FUNCTION OF FILTER MEDIUM

In Cake Filtration

Ideally a filter medium allows unrestricted passage of a fluid through its pore structure while retaining all suspended solid particles originally present in the fluid. The solid particles may be retained entirely at the surface of the filter medium if all particles are larger than the pores of the medium and the pore structure of the medium consists of simple, straight-through pores of nearly equal size. While this case may be approximated in a simple screening operation on a plain mesh screen or by filtration through colloidal membranes, the usual filtration case is much more complex. Most chemical suspensions as filtered contain ultimate particles of subsieve and often submicron size, which may be well dispersed or partially or highly flocculated depending on the solids concentration in the suspension and the chemical nature of the suspending solution. In almost all practical cases a fairly wide range of effective particle size exists in the feed, either as a result of a wide ultimate particle-size distribution and/or a condition of partial flocculation of the ultimate particles. Thus, in the usual case the pore structure of the filter medium must remove particles of over a hundredfold size range without unduly restricting fluid flow.

The problem is further complicated by the limitations placed on the pore structure of the medium by the method of construction. Woven fabrics used for cake filtration have relatively large interyarn pores in parallel with much smaller interfiber pores. Both types of pores tend to present a passage of greater tortuosity than a straight-through pore and both vary in size throughout their length. In packed beds of fibers (woven or pressed felts, fibrous filter aids, etc.) and in packed beds of rigid particles (sintered-

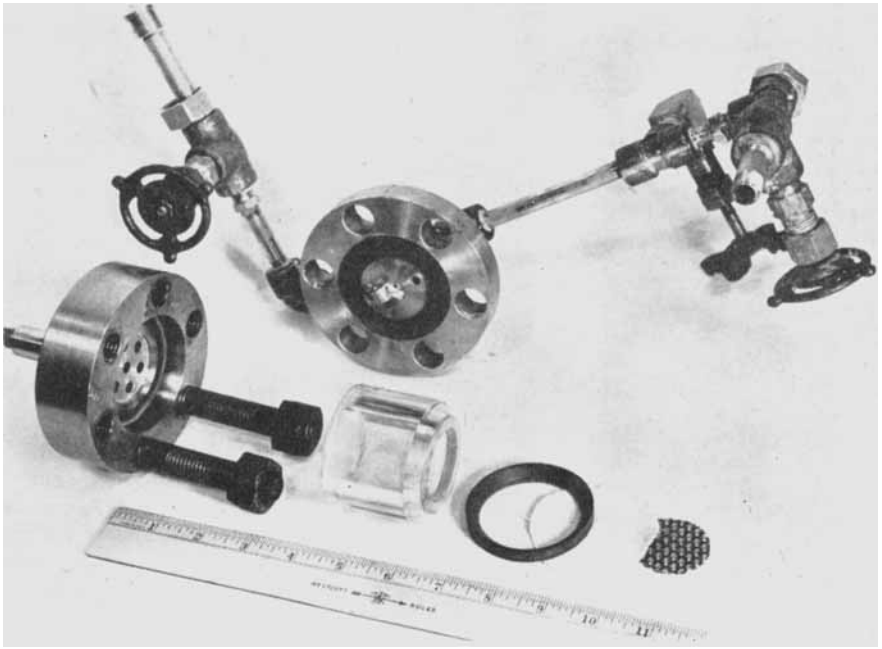

Fig. 1. Apparatus used to make filtration runs: top, pressure-filter cell; bottom, assembled filtration and recording apparatus.

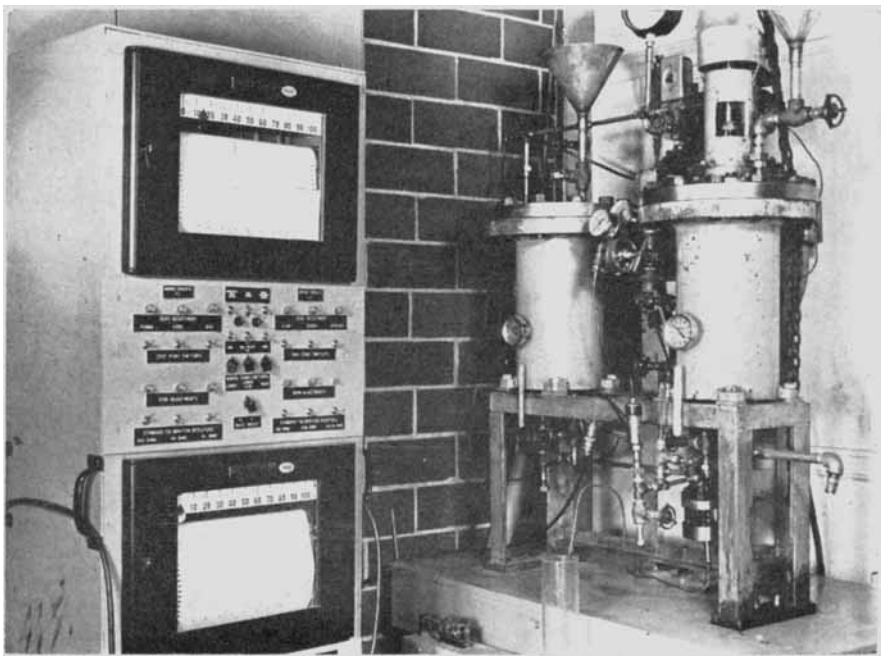

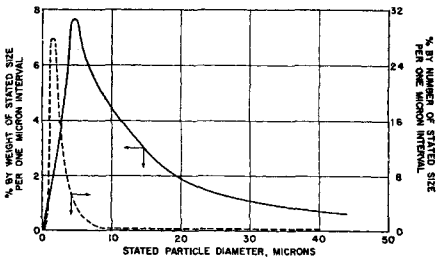

Fig. 2. Particle-size distribution of spherical particles filtered.

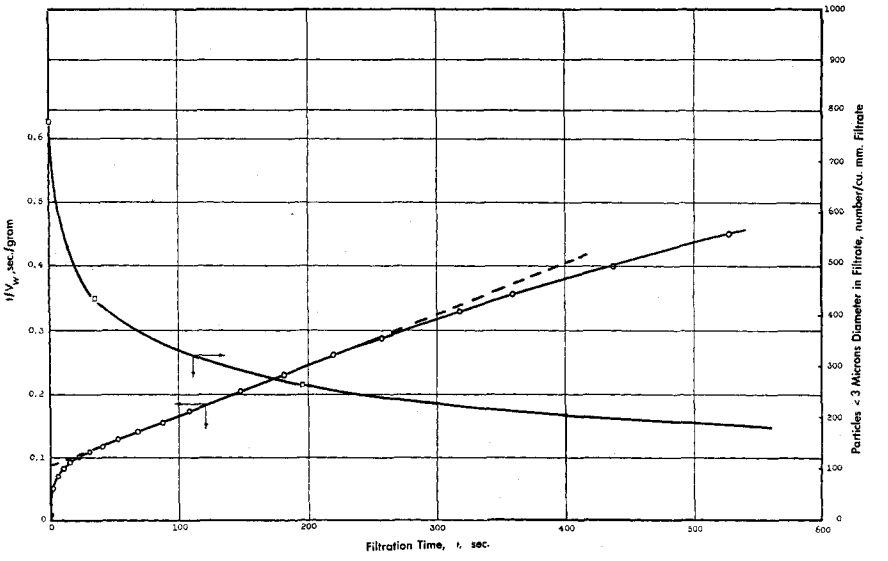

Fig. 3A. Initial portion of filtration run with 175-TW cotton twill.

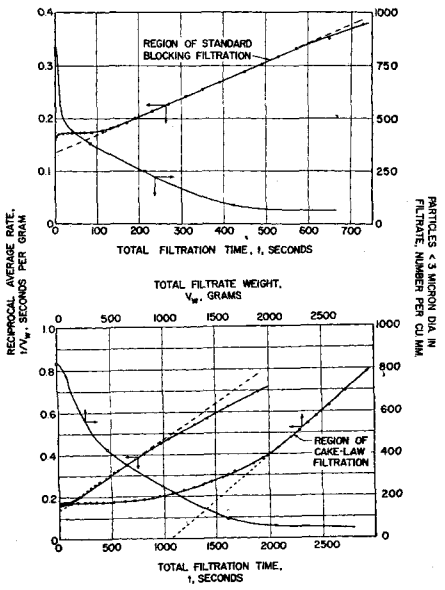

Fig. 3B. Over-all filtration run with 175-TW cotton twill.

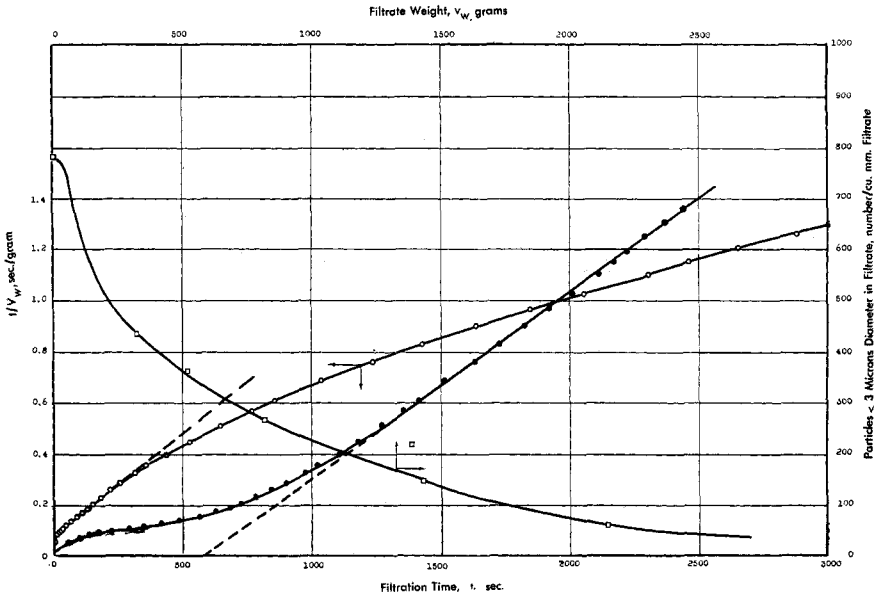

Fig. 4. Filtration performance curves FE-420 Orlon satin. Above: ○ t/V_w vs. t, □ particle count vs. t; below: ○ t/V_w vs. t, ● t/V_w vs. V_w, □ particle count vs. V_w.

metal or ceramic media, particulate filter aids, etc.) the tortuosity of pore structure is even greater, but a random distribution of pore volume exists throughout the medium although interconnecting pores probably contract and expand continually along any path through the medium.

When filtering suspensions contain more than 1% by volume solids (*cake filtration*), the pores block with cake in the first few seconds or fraction of a second and a continuous cake covers the surface of the filter medium. This cake immediately becomes the active filter surface, and particle passage through, or penetration of, the filter medium, which causes plugging of the medium, occurs for only a very short period at the start of each successive filtration cycle. Although of short duration, this repetitive plugging period eventually results in blinding of the filter medium, thus limiting its useful life. Very little is known concerning the mechanisms of this short plugging period or the initial stages of cake formation at the surface of the filter medium.

Many workers have demonstrated that the effective resistance of the filter medium during cake filtration is considerably greater than the resistance of the medium alone either before a filtration or after cake discharge at the end of a cycle; this work is well summarized by Ruth (*17*) and Carman (*1*). The effective filtration resistance is determined by extrapolation to $V/A = 0$ of the usual $\Delta t/\Delta(V/A)$ vs. V/A plot of constant-pressure data for cake filtration (*17*). Actually such a plot is no longer a straight line near $V/A = 0$, and mechanisms other than increasing resistance due to cake formation alone become controlling. Previously reported work (*6*) has shown that the effective resistance of a given medium in cake-filtration service depends on both the system and the filtration pressure but is generally equal to the resistance of a 0.01- to 0.06-in. thickness of cake under the same conditions. Many workers, including Ruth (*17*), Heertjes and Haas (*7*), and Hixson, Work, and Odell (*10*), have postulated the mechanism of particle bridging at the start of cake filtration. Although Hixson et al. were able experimentally to demonstrate bridging by means of glass capillaries and highly concentrated quartz suspension, there is no conclusive evidence that bridging is a major factor in most industrial filtrations involving cake formation. General expe-

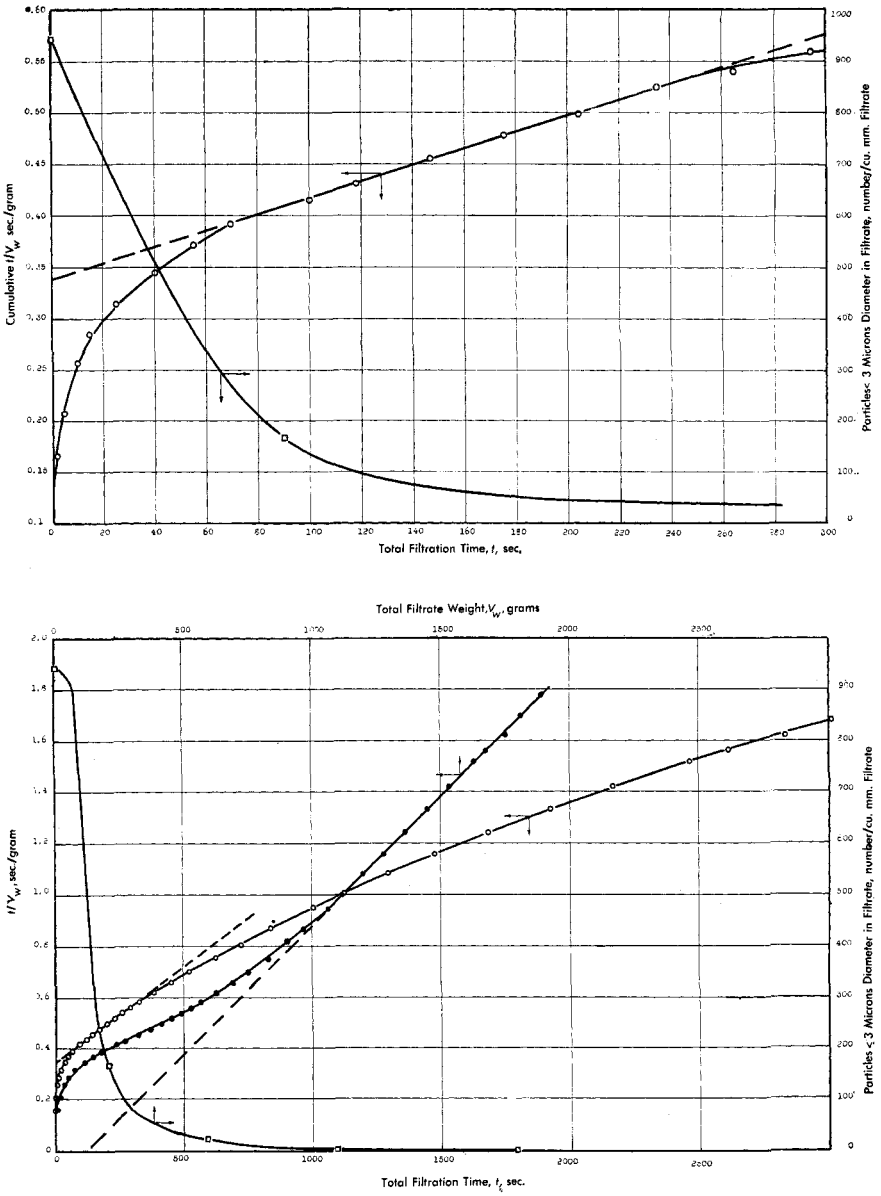

Fig. 5. Filtration performance curves SN-23 spun nylon. Above: ○ t/V_w vs. t, □ particle count vs. t; below: ● t/V_w vs. V_w, ○ t/V_w vs. t, □ particle count vs. V_w.

rience has shown that both initial filtration pressure and solids concentration have great influence on the effective resistance of the filter medium. Smith (*19*) has stated that for a given system and filter medium a critical pressure drop exists for each solids concentration and that if this is exceeded bridging fails to occur and severe plugging of the filter medium results. Although it is recognized that excessive filtration pressure drop can cause serious plugging of the medium at the start of filtration with certain highly compressible cakes, there is no direct experimental evidence that a critical pressure drop exists. The postulated failure of bridging may be correct; however, the plugging may just as likely be due to breakdown of floc structure (compressible cakes result from filtering of highly flocculated suspensions) at the surface of the filter medium under the intense shear at the pore openings; such breakdown of floc would result in increasing penetration and plugging of the filter medium by a smaller effective size of particle as the initial pressure drop is increased.

The lack of knowledge concerning the mechanisms occurring during the initial period of cake filtration results largely from the extremely short duration of this critical period. An important practical consequence is the difficulty of determining, on a laboratory scale, the relative-performance characteristics of several media for a particular cake filtration. The running of a protracted series of cake-filtration cycles has been recommended, but at best this method is laborious and yields data which have meaning only with the exact conditions and system employed. As the solids concentration in the feed suspension is decreased below 100 p.p.m. (0.01%) by volume, the duration of the initial period of filtration before formation of a cake is extended to such an extent that study of the mechanisms involved becomes practical. It seems very probable that essentially the same mechanisms may occur at higher solids concentrations with only the relative time duration of the mechanisms varying; this assumes that the effective particle size of the system is not changed by flocculation. An attempt to apply this approach was made by Heertjes and Haas (*7*); however, most of their work dealt with particles which were so large that they did not tend to penetrate and plug the filter media used.

In Solution Clarification

The filtration of dilute suspensions containing less than 100 p.p.m. by volume of solids is in its own right of great practical importance. For economical

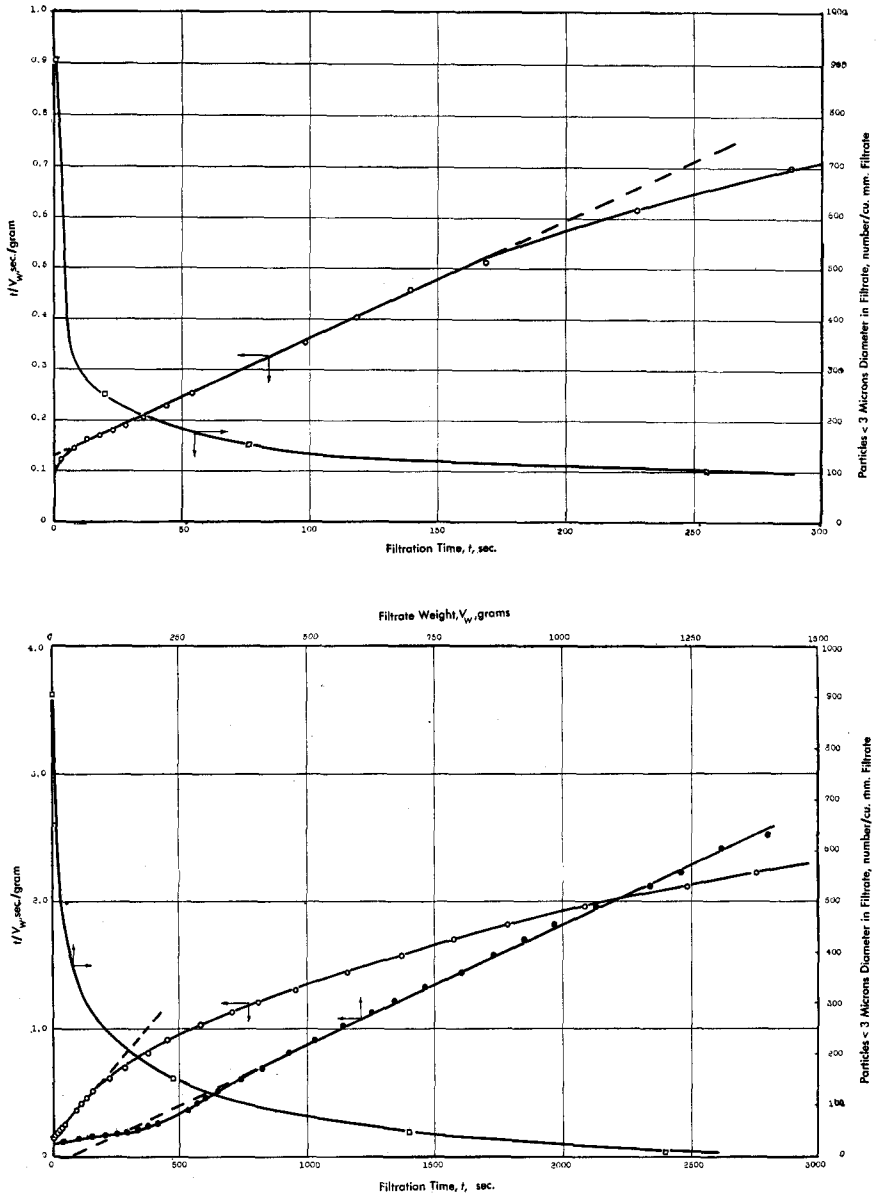

Fig. 6. Filtration performance curves TF-5044 filament nylon twill. Above: ○ t/V_w vs. t, □ particle count vs. t; below: ● t/V_w vs. V_w, ○ t/V_w vs. t, □ particle count vs. V_w.

reasons such filtrations normally include only that portion of the filtration cycle preceding cake formation. Operation into the region of cake filtration is usually impractical because of the very high resistance of the cake deposited. This results from the much better particle dispersion existing in such dilute suspensions and also, in several important cases, from the fact that the particles being removed are true gels having a very deformable structure. Thus in solution-clarification operations the purpose of the filter medium is to allow penetration but to trap individual particles within the structure of the medium with the least increase in medium resistance to flow per volume of particles trapped. Unlike the practice with cake filtration, stopping of particles at the surface of the medium is not desirable, and the objective is a long life during a single filtration cycle rather than a long life in terms of many cycles, as in cake filtration. Despite this basic difference in the over-all objective, the ultimate service life, as limited by plugging and increased resistance, depends in both cases on that portion of the filtration cycle preceding cake formation. It therefore appears that performance evaluation of filter media employing dilute suspensions may serve to characterize the performance of a filter medium in both cake-filtration and solution-clarification services.

MECHANISMS OF PARTICLE REMOVAL IN CLARIFICATION

In addition to (*a*) the direct-sieving action at constrictions in the pore structure, other possible mechanisms of particle collection within the filter medium are (*b*) gravity settling, (*c*) Brownian diffusion, (*d*) interception at the solid-liquid interfaces, (*e*) impingement, and (*f*) electrokinetic forces. Expressions for estimating the relative magnitudes of (*b*) to (*e*) under various conditions have been reported by Langmuir (*13*), Thomas (*20*), and Davies (*3*) and applied in gas filtration. Calculations employing these expressions and based on a range of filtration conditions for removal of 0.5- to 20-μ particles from liquids suggest that (*b*), (*c*), and (*e*) are negligible compared with (*d*), the direct interception of particles from liquid streamlines in contact with pore walls. In general, the relative importance of (*d*) with respect to (*b*), (*c*), and (*e*) increases as the liquid viscosity increases. The relative impor-

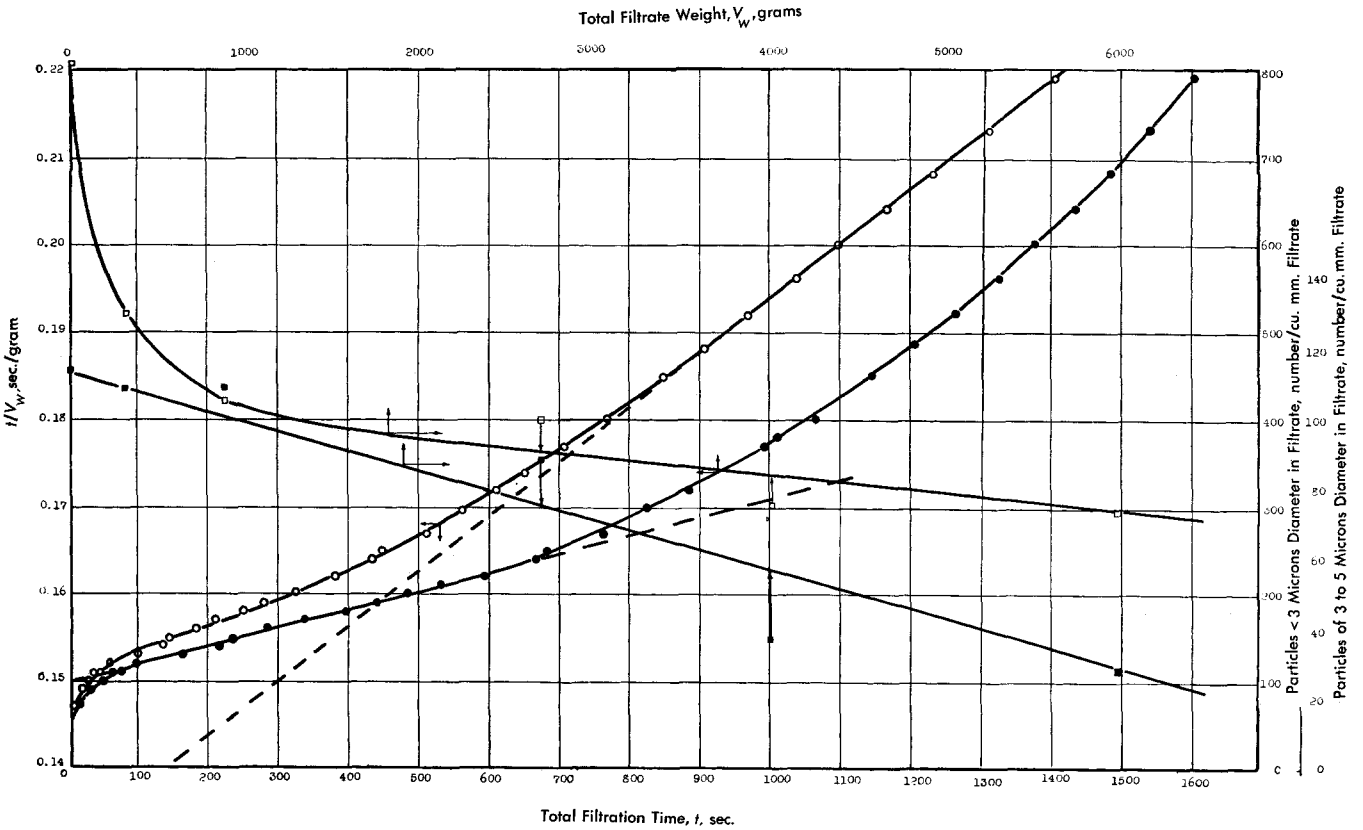

Fig. 7. Filtration performance curves AF-220 woven wool felt: ● t/V_w vs. V_w, ○ t/V_w vs. t, □ <3 μ particle count vs. V_w, ■ 3 to 5 μ particle count vs. V_w.

tance of this direct-interception mechanism to direct sieving action at constrictions in the pore structure and to electrokinetic forces cannot be estimated at this time. Also, the effectiveness of particle retention after collection has been accomplished is a factor which is little understood. Data for gas filtration (*20*) show that retention decreases as gas velocity (and also pressure drop) increases. Whether increased viscosity (with velocity constant and pressure drop increasing) will decrease retention has not been established for either gases or liquids.

The basic differences between the controlling mechanisms of particle collection in the clarification of gases and the clarification of liquids result either directly or indirectly from the much greater liquid viscosity. The direct effect of a higher filtrate viscosity on the relative importance of the several collection mechanisms has already been noted. Indirectly a higher filtrate viscosity results in the use of media of much lower porosity (0.30 to 0.70 void fraction for liquid clarification as compared with 0.90 to 0.99 void fraction for gas clarification). This comes about because media of higher porosity, such as packed beds of fibers, become so compressed by the resulting pressure drop when filtering liquids at practical rates that they are no longer high-porosity media under actual filtration conditions with liquids. Rodebush (*16*) has reported that for gases a decrease in medium porosity results in an increase in the collection coefficient, but that such an increase is accompanied by a correspondingly larger increase in flow resistance. On this basis the low porosities of media used for liquid filtration appear undesirable, but necessary until a completely rigid medium of very high porosity can be devised. On a theoretical basis an increase in collection efficiency with decreasing porosity cannot be accounted for on the basis of collection mechanisms (*b*) to (*e*) above, as the basic number of targets is not changed by compression of the medium. However, as compression occurs and porosity decreases, the filter appears less and less like a field of targets and more and more like a barrier with interconnecting pores or passages. As this occurs, collection by direct sieving at pore constrictions becomes increasingly important and probably accounts in part for the reported increase in collection coefficient with decreasing porosity. In any case most liquid clarifications are carried out with media having low enough porosities so that they can best be thought of as barriers with an interconnecting pore structure, rather than as an open field of targets as is the case in most gas clarifications.

LAWS AND MECHANISMS OF PORE PLUGGING DURING FILTRATION OF DILUTE SUSPENSIONS

Hermans and Bredée (*8*), and more recently Gonsalves (*4*), have analyzed the entire filtration cycle and proposed a series of laws to correlate the filtration-rate data for various parts of it. The mathematical expressions for these laws are summarized in various forms in Table 1. These filtration laws were derived by Hermans and Bredée on the assumption of separate physical mechanisms of pore plugging for complete blocking, standard blocking, intermediate blocking, and cake modes of filtration. However, Gonsalves (*4*) has shown that these same laws can also be derived on the assumption of quite different physical mechanisms for the blocking of pores within the medium; thus even though the mathematical expressions for these laws fit the experimental data for certain parts of the filtration cycle, there is no real evidence as to what the actual physical mechanism of pore blocking may be. The work of Hermans and Bredée and of Gonsalves has shown, however, that all the derived relationships stem from a common differential equation which can be adapted to any portion of the filtration cycle by adjusting the values of two constants. Thus, for constant-pressure filtration,

$$\frac{d^2t}{dV^2} = k\left(\frac{dt}{dV}\right)^n \qquad (1)$$

and for constant-rate filtration

$$\frac{d(\Delta p)}{dV} = k(\Delta p)^n \qquad (2)$$

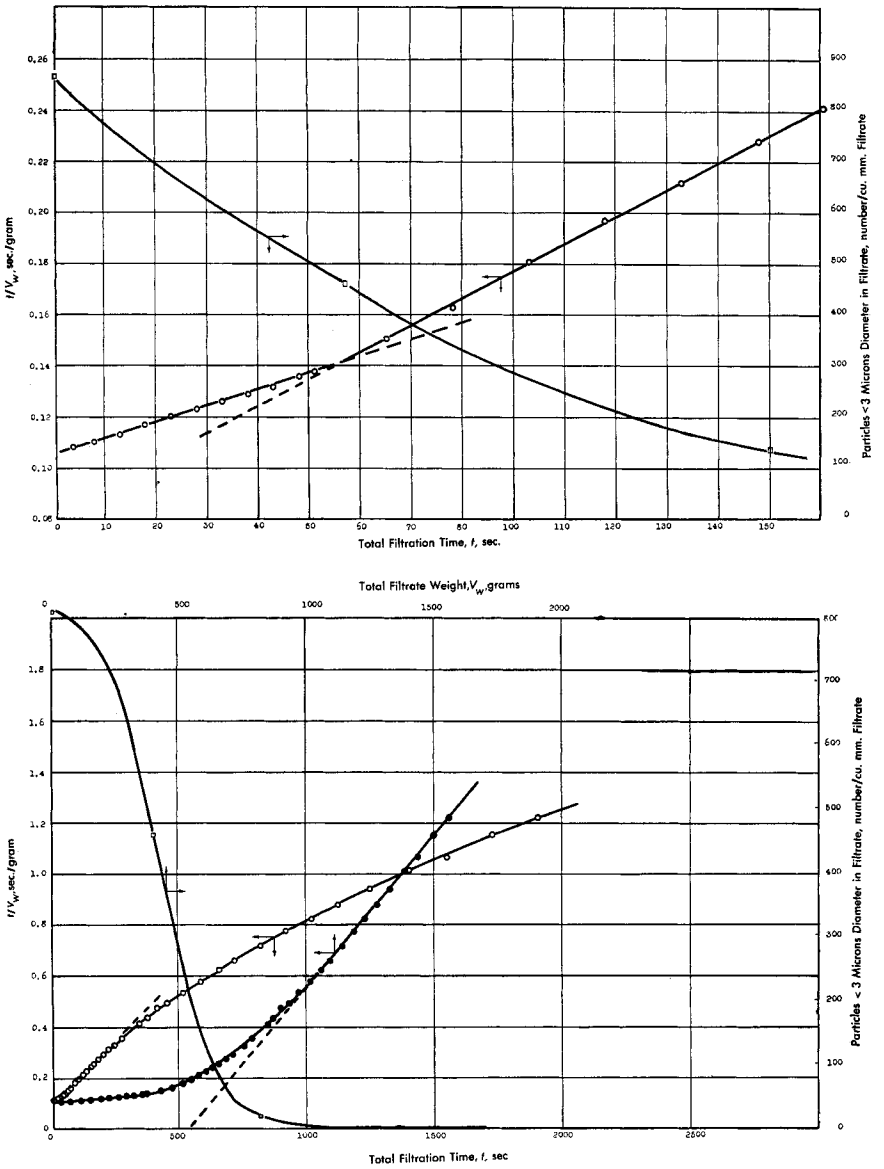

Fig. 8. Filtration performance curves TF-5071 Orlon taffeta, not calendered. Above: ○ t/V_w vs. t, □ particle count vs. t; below: ● t/V_w vs. V_w, ○ t/V_w vs. t, □ particle count vs. V_w.

where the value of n defines the mode of filtration occurring, and the value of k for a particular mode of filtration depends on the system, the filter medium, and the conditions of filtration. In simple terms, Equations (1) and (2) state that the rate of change of filter resistance is proportional to the instantaneous filtration resistance raised to a power which is dependent on the mode of filtration. The mode of cake filtration is well established, and for this case $n = 0$. Integration of Equation (1) at constant pressure drop for $n = 0$ gives

$$\frac{t}{V} = \frac{K_c V}{2} + \frac{1}{q_0} \qquad (3)$$

where

$$K_c = (1.56 \times 10^{-7}) \frac{\mu_f \alpha w}{A^2 g_c \Delta p_0} \qquad (4)$$

$$\frac{1}{q_0} = (4.74 \times 10^{-4}) \frac{\mu_f R_m}{A g_c \Delta p_0} \qquad (5)$$

The mode of standard blocking, although not so well established experimentally as cake filtration, has been found to fit the data for a significant portion of the filtration cycle with many dilute suspensions. Hermans and Bredée (*8*) cited examples of this mode of filtration as occurring in the filtration of polymer solutions, dispersed pigments, and cellulose solutions such as viscose and cellulose acetate. For this mode of filtration, $n = 3/2$ and integration of Equation (1) at constant pressure gives

$$t/V = \frac{K_s}{2} t + \frac{1}{q_0} \qquad (6)$$

The physical assumption made in the derivation of this relationship is that of particle retention at the walls of the pores and gradual build-up on pore walls with eventual plugging of the pores. Such a physical concept represents a constantly decreasing pore size in the filter medium and is in agreement with Kane's (*11*) more recent analysis of performance data on one commercial type of filter cartridge for clarifying liquids. The form of the standard-blocking relationship shown in Equation (6) has been widely used to correlate data for the filtration of viscose and cellulose acetate through various types of filter media which function by filtration in depth. As applied to the evaluation of viscose filterability in Europe, the German Standard Method assumes that Equation (6) applies from near the start of filtration for this particular case and K_s is solved for directly without plotting of t/V vs. t, by use of filtrate volumes collected after 20- and 60-min. filtration. Several European workers (*9*, *14*, *15*, and *21*) have recently recognized that Equation (6) does not apply for an initial period of filtration even with viscose and have recommended more care in the industrial use of Equation (6). Applying improved techniques, these same workers have investigated the effect of both viscose preparation and the filter medium used on the region over which Equation (6) applies. These workers suggested many reasons for the failure of Equation (6) at the start of the first stage of viscose filtration or when viscose is refiltered at later stages, but none have been satisfactorily verified. In plant practice such clarifications are often carried out at constant rate rather than constant pressure.

The constant-rate form of the standard-blocking law, as is needed to correlate such constant-rate filtration data, can be written in the form

$$\left(\frac{\Delta p_0}{\Delta p}\right)^{1/2} = 1 - \frac{(K_s)}{(2)} V \qquad (7)$$

Equation (7) has been observed to fail near the start of filtration, as has Equation (6).

The complete-blocking ($n = 2$) and intermediate-blocking ($n = 1$) modes of filtration as proposed by Hermans and Bredée have been found to have much more limited application. In general the regions of the filtration cycle to which these modes of filtration apply are ill-defined and of short duration, although a few systems involving only particles of size larger than the pores of the medium appear to follow the complete-blocking mode of filtration. The mathematical expressions for these modes, as derived by Hermans and Bredée for constant-pressure and constant-rate filtrations, are given in Table 1.

Recently both Gonsalves (*4*) and Vosters (*22*) have reanalyzed the work of Hermans and Bredée, raising the question as to whether several distinct

modes of filtration exist (as characterized by fixed values of n) before cake formation. Gonsalves has further questioned the physical mechanisms assumed in Hermans and Bredée's derivations, and has suggested trial-and-error solution of Equation (1) for simultaneous determinations of both k and n values which best fit a particular set of data for filtration before cake formation. This is a laborious process and the results are not particularly informative on a comparative basis because both k and n are generally different for filtrations under different conditions. Essentially what Gonsalves (*4*) has attempted is to find a single solution of Equation (1) over the entire filtration cycle preceding cake formation. On the other hand, Vosters (*22*), in an attempt to improve the reproducibility of the plugging-constant method of evaluating viscose, has resorted to calculation of a statistical straight line through the t/V vs. t values over a 50-min. period of constant-pressure filtration. For plant-control work, Vosters then uses the plugging constant as the tangent of the regression line, t/V on t. This approach ignores the real shape of the curve and is unsuited to interpretation of the real meaning of changes in the t/V vs. t curve. Although the filtration data of both Gonsalves and Vosters, like those of many other workers, do not follow the standard-blocking mode ($n = 3/2$) at the start of filtration, they, like those of most others, do so over a significant part of the remaining filtration cycle before cake formation. Thus, although Gonsalves' and Vosters' criticisms of indiscriminate application of the standard blocking mode ($n = 3/2$) as a means of analyzing filtration data from the very start of filtration are justified, complete discard of the idea that a definite standard-blocking mode ($n = 3/2$) exists does not yet appear justified.

The physical assumptions and derivation of the equations for the standard-blocking mode are presented in the Appendix. Derivation of the relationships has been carried a step beyond that of Hermans and Bredée (*8*). This has been done in an effort to express the relationships entirely in terms of the filter-medium properties. This has resulted, for constant-pressure filtration, in the form

$$t/V = (1.42 \times 10^{-4}) \frac{(8h)}{(\pi N r_0^4)} \frac{(\mu_f)}{(A g_c \Delta p)} + \left[\frac{c/(1-\epsilon_p)}{\pi N A h r_0^2}\right] t \quad (8)$$

and, for constant-rate filtration, in the form

$$\left(\frac{\Delta p_0}{\Delta p}\right)^{0.5} = 1 - \left[\frac{c/(1-\epsilon_p)}{\pi N A h r_0^2}\right] V \quad (9)$$

Thus, in either case a solution for the clogging value $\pi N h r_0^2$ should be possible from filtration data provided that the standard-blocking mode applies to a portion of the filtration cycle, resulting in a straight-line region for a t/V vs. t or a $(\Delta p_0/\Delta p)^{0.5}$ vs. V plot of the data. For such a straight-line region to exist, the degree of particle-size retention, or the value of c, must remain substantially constant, and unless the retention is essentially complete ($c = c_f$), the amount of bleed, $c_f - c$, must be known. This fact has been largely overlooked in the application of Equation (6) by most workers and may account for the generally reported failure of Equation (6) at the start of filtration. Solution of Equations (8) and (9) for comparative values of the clogging value $\pi N h r_0^2$ with various filter media, under similar filtration conditions and with the same suspension, offers a means of quantitatively comparing the plugging characteristics of various media. If the values of $\pi N h r_0^2$ so determined could be related to independently measured dimensions of the pores in the media, then a quantitative link might also be established between the plugging characteristics of a medium and its internal pore structure.

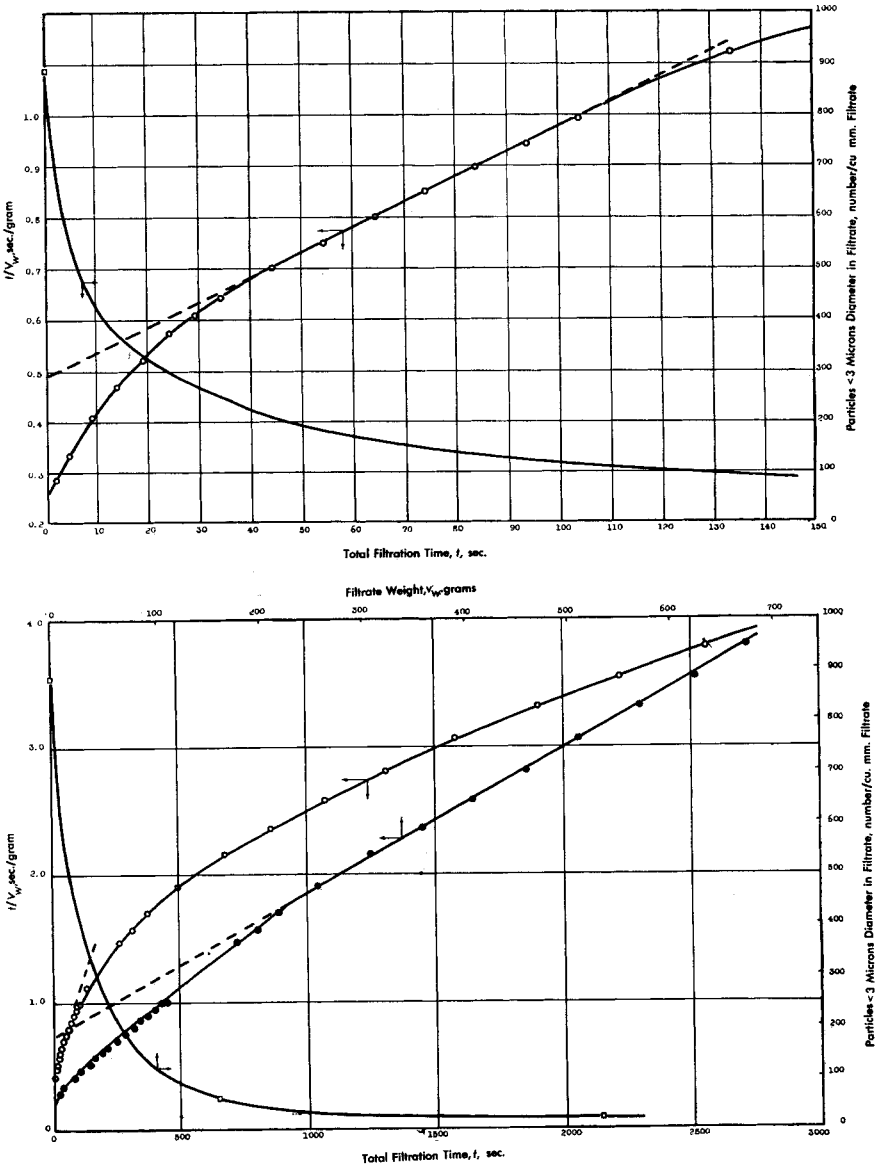

Fig. 9. Filtration performance curves TF-5071-F Orlon taffeta, calendered. Above: ○ t/V_w vs. t; below: ● t/V_w vs. V_w, ○ t/V_w vs. t, □ particle count vs. V_w.

EXPERIMENTAL EQUIPMENT AND PROCEDURES

Equipment

The equipment shown in Figure 1 was used to obtain comparative filtration data for various filter media by use of a dilute suspension of known particle-size distribution. The filtration cell (Figure 1*a*) was of 11.35 sq. cm. filtration area. The filter medium was clamped over an 8-mesh

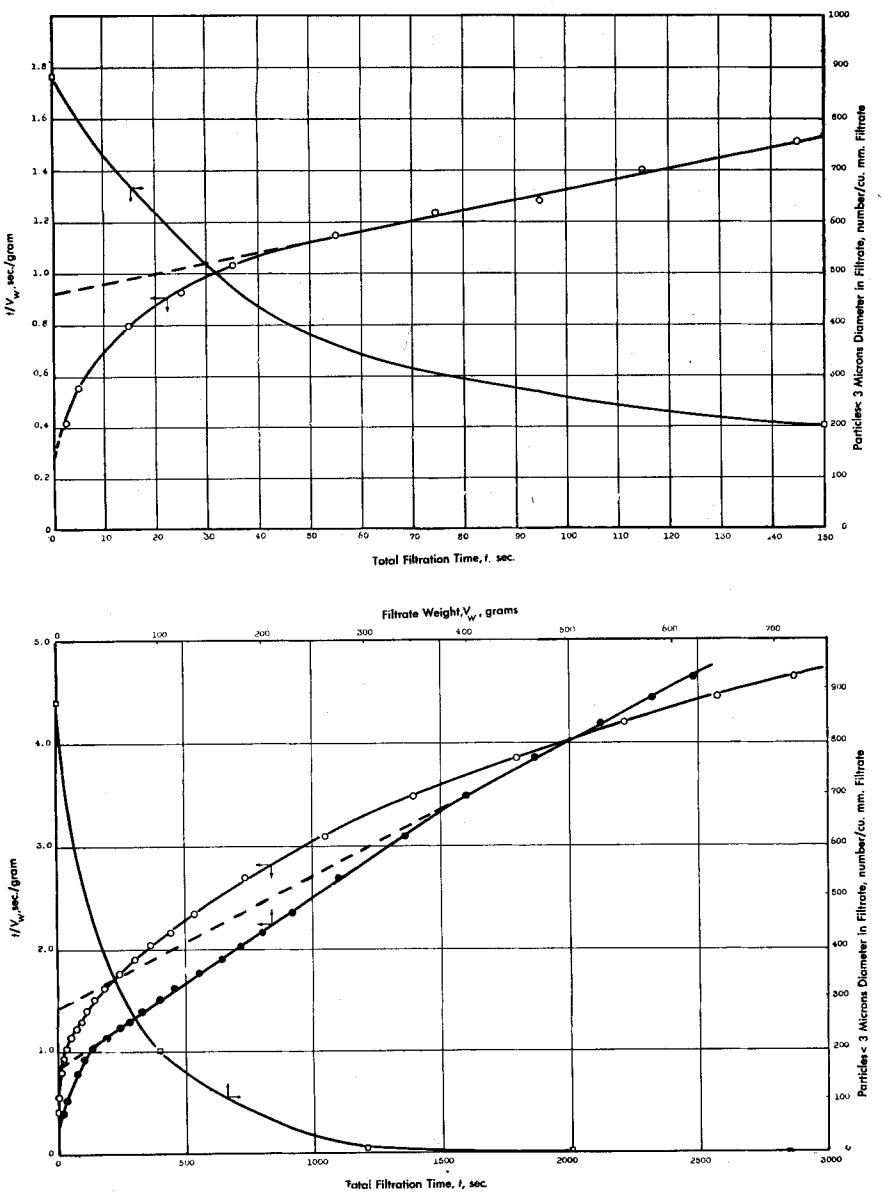

backing screen. The 20 p.p.m. by volume feed suspension was fed to the filtration cell from the agitated blow case (Figure 1*b*) at constant pressure drop. Filtrate weight, pressure drop, and filtrate temperature were recorded continuously by the automatic recording system. The all stainless steel piping and equipment were thoroughly cleaned before use and maintained uncontaminated by other than the feed suspension throughout the experimental program.

Filtration Runs

The suspension system used for the filtration runs consisted of an 80% glycerol–20% water solution containing approximately 0.18 g./liter (23 p.p.m. by volume) of spherical particles of carbonyl iron powder. The carbonyl iron powder used was a mixture of three commercial grades made by the Anatara Products Division of General Aniline & Film Corp. The particles were very nearly all of spherical shape, facilitating microscopic counting of size. The powder mixture was first dispersed in 0.01M $Na_4P_2O_7$ solution by 1-hr. agitation, following which C. P. white glycerol was added with agitation to make the final suspension. The particle-size-distribution function of the powder mixture is shown in Figure 2. The weight-frequency distribution curve was calculated from the sedimentation analysis of individual grades present in the mixture. The number-frequency-distribution curve was determined directly by microscopic count of suspension samples (Figure 2). Similar number-frequency-distribution curves have recently been reported

Fig. 10. Filtration performance curves No. 8 cotton duck. Above: ○ t/V_w vs. t, □ particle count vs. t; below: ● t/V_w vs. V_w, ○ t/V_w vs. t, □ particle count vs. V_w.

TABLE 1. FILTRATION LAWS OF HERMANS AND BREDÉE (8)

1. For constant-pressure filtration

Function	Complete blocking	Standard blocking	Intermediate blocking	Cake filtration
$\frac{d^2t}{dV^2} = k\left(\frac{dt}{dV}\right)^n$	$n = 2$	$n = 3/2$	$n = 1$	$n = 0$
$V = f(t)$	$V = q_0(1 - e^{-k_b t})$	$t/V = \frac{K_s}{2}t + \frac{1}{q_0}$	$K_i V = \ln(1 + K_i t q_0)$	$t/V = \frac{K_c}{2}V + \frac{1}{q_0}$
$q = f(t)$	$q = q_0 e^{-K_b t}$	$q = \frac{q_0}{\left(\frac{K_s}{2}V + 1\right)^2}$	$K_i t = \frac{1}{q} - \frac{1}{q_0}$	$q = \frac{q_0}{(1 + K_c q_0^2 t)^{1/2}}$
$q = f(V)$	$K_b V = q_0 - q$	$q = q_0\left(1 - \frac{K_s V}{2}\right)^2$	$q = q_0 e^{-K_i V}$	$K_c V = \frac{1}{q} - \frac{1}{q_0}$

2. For constant-rate filtration

$\frac{d(\Delta p)}{dV} = k(\Delta p)^n$	$n = 2$	$n = 3/2$	$n = 1$	$n = 0$
$\Delta p = f(V)$	$\frac{\Delta p_0}{\Delta p} = 1 - \frac{K_b V}{q_0}$	$\left(\frac{\Delta p_0}{\Delta p}\right)^{0.5} = 1 - \left(\frac{K_s}{2}\right)V$	$\ln\left(\frac{\Delta p}{\Delta p_0}\right) = K_i V$	$\frac{\Delta p}{\Delta p_0} = K_c q_0 V + 1$
$\Delta p = f(t)$	$\frac{\Delta p_0}{\Delta p} = 1 - K_b t$	$\frac{1}{q_0}\left(\frac{\Delta p_0}{\Delta p}\right)^{0.5} = \frac{1}{q_0} - \left(\frac{K_s}{2}\right)t$	$\frac{1}{q_0}\ln\left(\frac{\Delta p}{\Delta p_0}\right) = K_i t$	$\frac{\Delta p}{\Delta p_0} = K_c q_0^2 t + 1$

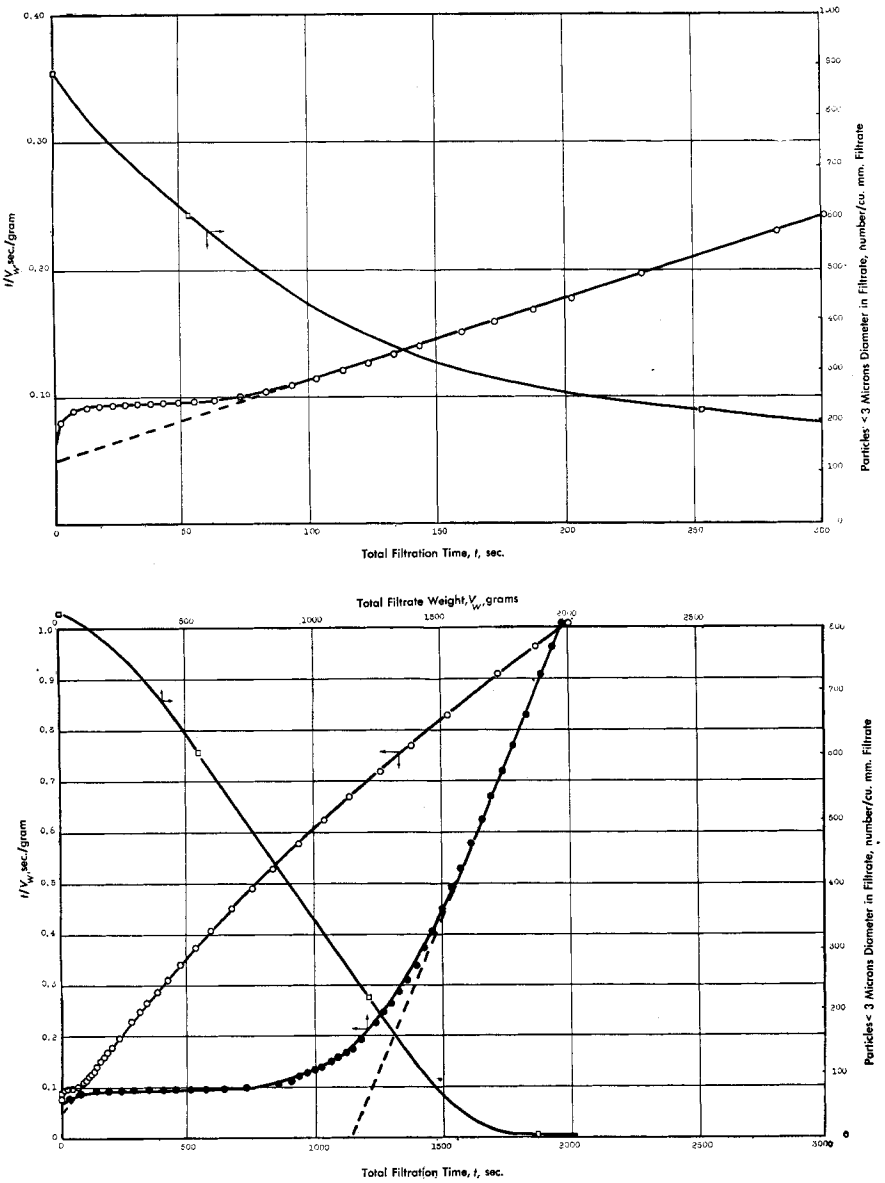

Fig. 11. Filtration performance curves WS SN-7 filament nylon duck. Above: ○ t/V_w vs. t, □ particle count vs. t; below: ○ t/V_w vs. t, ● t/V_w vs. V_w, □ particle count vs. V_w.

for individual grades of similar carbonyl iron powders by Kohl and Zentner (*12*).

Constant-pressure-filtration runs were made with nine of the filter media previously examined by the mercury-intrusion method (Part I of this paper). Pieces cut from the same filter-medium sample were used for both mercury-intrusion and filtration measurements. The filtration runs were made at room temperature by use of the feed suspension and equipment just described. A constant pressure drop in the range of 14 to 15 lb./sq. in. was maintained during each run. At the start of filtration, air was bled out the top of the filtration cell before filtration started. Filtrate holdup volume between the filter medium and the strain-gauge scale was 6 ml.; this volume was filled with solution before filtration started so that filtrate collection and filtration started simultaneously. Grab samples of filtrate of 50-ml. volume were taken periodically throughout the run for filtrate analysis. These samples were noted on the recorder chart and taken into account in analyzing the filtrate-weight vs. time data. The filtrate container on the strain-gauge scale was changed for every 500 to 1,000 g. of filtrate collected; these larger composite samples of filtrate were also analyzed for solids content, as was a sample of the feed suspension at the start of filtration. Filtrate viscosity at the run temperature was determined in each case by use of the Hoeppler falling-ball viscometer. Duration of the filtration runs was from 1,400 to 3,600 sec., depending on the filter medium employed. It was generally apparent that the $t - V_w$ data had begun to follow the cake-filtration law before each filtration was stopped. However, in the case of Albany 220 felt this condition was not achieved before the blow case was emptied. At the end of each run the filter medium was removed and examined microscopically on both cake and filtrate sides.

Filtrate Evaluation

The samples of suspension feed, grab samples of filtrate, and composite samples of filtrate taken during each filtration run were examined microscopically and particle counts made for the < 3, 3-5, 5-10, 10-15 and > 15μ size ranges. A Howard mold counting cell was used and provided a sample depth of 0.10 mm. Counts were made at 200 X magnification by use of binocular eyepieces and a calibrated counting grating. Counts were made about 10 min. after the sample was placed in the Howard mold counting cell; this provided time for iron particles to settle through the 0.10 mm. depth of cell and facilitated counting since all particles were in essentially the same plane and were at rest. In general, several scans were made across various diameters of the circular-mold counting cell (18.5 mm. diam.). For most samples the total number of particles counted was in the range of 100 to 1,000, with 85 to 100% of the particles being smaller than 3μ, for the various samples. The concentration of the various feed suspensions (Table 2) was determined gravimetrically by filtering on weighed Gooch crucibles with asbestos pads, the volumetric concentration being calculated from the particle density of 7.81 g./cc.

DISCUSSION OF RESULTS

Limitations Found in the Application of the Filtration Laws

Data from the filtration runs on the nine filter media are first analyzed in terms of the t/V_w vs. t and t/V_w vs. V_w curves of Figures 3 to 11. These curves are shown for the entire run and are also plotted on an expanded scale for the portion of the cycle preceding cake-law filtration. The straight-line portions of these curves fully define the regions of both standard blocking and cake filtration, in accordance with Equations (3) and (6). Also plotted on these same Figures 3 to 11 for the various filter media are curves of particle count in the filtrate vs. V_w or t.

In general, the data for all media exhibit an initial region of filtration during which neither the standard-blocking nor cake-filtration modes apply. Over this initial region a large number of feed particles appear in the filtrate, and this number decreases very rapidly as filtration proceeds. Following this, a transition into a region of standard blocking appears to occur with all media except the Albany 220 felt. The duration of this region of standard blocking varies depending on the character and tightness of the filter medium, being longest for loosely woven media of staple fibers such as 175-TW cotton twill (Figure 3) and shortest for tightly woven and calendered media of multifilament construction such as TF-5044 (Figure 6) or TF-5071-F (Figure 9). However, the standard-blocking period is also of short duration with a tightly woven medium of staple fibers, such as No. 8 cotton duck (Figure 10). With the other media of staple or multifilament construction the period of standard blocking was of intermediate duration. With the Albany 220 felt (Figure 7) the initial region of filtration

TABLE 2. SUMMARY OF PLUGGING COEFFICIENTS AND CAKE-RESISTANCE VALUES CALCULATED FROM FILTRATION RUNS

				Region of standard blocking (From t/V_w vs. t data plots)				Region of cake filtration (From t/V_w vs. V_w data plots)				
				Straight line				Straight line				
Filter-media style	Pressure drop, Δp, lb./sq. in.	Filtrate viscosity, μ_f, centipoises	Solids concentration, c, p.p.m. by vol.	Slope, $K_s/2$, 1/g.	Intercept, $1/q_0$ sec./g.	Clogging value $\pi N h r_0^2$, cc./sq. cm.	Pore resistance $8h/\pi N r_0^4$, 1/cm.	Slope, sec./g.^{2}	Intercept, sec./g.	Avg. specific cake resistance, α, ft./lb.	$\Delta t/\Delta V_w$ at start of cake-filtration region, sec./g.	Effective cloth resistance at start of cake filtration R_m, 1/ft.
175-TW Cotton twill	14.85	35.9	20.8	0.333×10^{-3}	0.137	83×10^{-4}	5.4×10^6	0.41×10^{-3}	−0.298	4.0×10^{10}	1.18	1.4×10^9
FE-420 Orlon, satin	14.5	30.4	22.1	0.79×10^{-3}	0.085	37×10^{-4}	3.8×10^6	0.73×10^{-3}	−0.423	7.7×10^{10}	1.41	1.92×10^9
SN-23 Staple nylon, duck	14.4	30.5	22.8	0.78×10^{-3}	0.340	39×10^{-4}	15×10^6	1.01×10^{-3}	−0.131	10.2×10^{10}	1.69	2.28×10^9
TF-5044 Filament nylon, twill	14.6	38.4	23.1	2.56×10^{-3}	0.130	12×10^{-4}	4.6×10^6	1.90×10^{-3}	−0.070	15.2×10^{10}	1.43	1.55×10^9
AF-220 Woven wool felt	14.2	32.4	21.9	6.75×10^{-5}	0.130	430×10^{-4}	5.4×10^6					
TF-5071-U Filament Orlon, taffeta	14.6	29.1	23.3	0.625×10^{-3}	0.106	50×10^{-4}	5.0×10^6	1.225×10^{-3}	−0.662	12.0×10^{10}	2.04	2.92×10^9
				1.04×10^{-3}	0.083	30×10^{-4}	4.0×10^6					
SN-7 Filament nylon, duck	14.8	26.4	22.8	0.637×10^{-3}	0.050	48×10^{-4}	2.6×10^6	1.37×10^{-3}	−1.55	16.4×10^{10}	2.27	3.40×10^9
TF-5071-F, Filament Orlon, calendered taffeta	14.8	28.2	23.0	4.88×10^{-3}	0.485	6.3×10^{-4}	25×10^6	6.87×10^{-3}	0.25		0.59	
								4.50×10^{-3}	0.74	50×10^{10}	3.08	4.60×10^9
No. 8 Cotton duck	14.5	27.4	22.6	4.12×10^{-3}	0.91	7.3×10^{-4}	46×10^6	6.60×10^{-3}	0.86		1.43	
								5.25×10^{-3}	1.40	60×10^{10}	5.65	8.55×10^9

$$t/V_w = \left(\frac{8h}{\pi N r_0^4}\right)\left(\frac{\mu_f}{\pi A \rho_f g_c \Delta p}\right) + \left(\frac{c/1-\epsilon_p}{\rho_f A \pi N h r_0^2}\right) t$$

$$\pi N h r_0^2 = \frac{(c_f/1-\epsilon_p)}{\rho_f A(\text{slope})} = \left(\frac{1}{11.35 \text{ sq. cm.}}\right)\left(\frac{c_f}{1-0.45}, \frac{\text{cc.}}{10^6 \text{ cc.}}\right)\left(\frac{\text{cc.}}{1.2 \text{g.}}\right)\left(\frac{1}{\text{slope}}, g\right) = \frac{1.33(10)^{-7} c_f}{\text{slope}}, \text{ cc./sq. cm.}$$

$$\left(\frac{8h}{\pi N r_0^4}\right) = \left(\frac{A \rho_f g_c \Delta p}{\mu_f}\right)(\text{intercept}) = 9.43(10)^7\left(\frac{\Delta_p, \text{ lb./in.}^2}{\mu_f, \text{ cp.}}\right)(\text{intercept, sec./g.}) = \frac{1}{\text{cm.}}$$

$$\alpha = \frac{2A^2 g_c \rho_f^2 \Delta_p}{\mu_f \rho_s c}(\text{slope}) = 4.88(10)^{15}\left(\frac{\Delta_p, \text{ lb./sq. in.}}{\mu_f, \text{ centipoises} \times c, \text{ p.p.m.}}\right)\left(\text{slope}, \frac{\text{sec.}}{\text{g.}^2}\right) = \text{ft./lb.}$$

$$R_m = \frac{A \rho_f g_c \Delta_p}{\mu_f}\left(\frac{\Delta t}{\Delta V_w} \text{ at start cake-filtration region}\right) = 28.6(10)^8\left(\frac{\Delta_p, \text{ lb./sq. in.}}{\mu_f, \text{ centipoises}}\right)\left(\frac{\text{sec.}}{\text{g.}}\right) = \frac{1}{\text{ft.}}$$

was followed by a brief region during which the cake-filtration law was apparently followed even though no cake existed on the surface of the felt. This in turn was followed by a prolonged period of standard-blocking behavior. This unusual behavior is similar to reported experiences in which the cake law may sometimes apply to the filtration of highly filtered solutions where no actual cake is formed and no apparent discoloration of the filter medium occurs. This unusual period of cake filtration was accompanied by passage through the filter medium of nearly half the number of particles originally present in the feed. With the Albany 220 felt (Figure 7) the period of standard blocking, which followed this pseudo cake filtration, continued until the end of the filtration run.

With all other media the period of standard blocking was followed by a transition region which yielded to a prolonged region of cake filtration; this continued until the end of the run. With very tight media such as the No. 8 cotton duck (Figure 10) and 5071-F calendered medium made from Orlon acrylic fiber, two regions of cake filtration occurred with an abrupt change in slope occurring at the transition from the first to the second. This transition resulted in a decrease in slope or a decrease in effective cake resistance. Only in the case of TF-5044 (Figure 6) was there any macroscopic evidence of cake formation at the end of the filtration run, although the surface of the filter medium was discolored in all cases. Figures 19 to 21 show photomicrographs of the filtrate side and cake side of the various filter media as removed at the end of the runs. It is evident that a true cake covering the entire surface of the filter medium was not formed in any case and that in most cases only a small part of the filter-medium surface is covered by a cake in even a microscopic sense. The successive regions of cake filtration with No. 8 cotton duck (Figure 10) and with TF-5071-F (Figure 9) may well result from changes in effective filtration area at the surface of the cake as the cake progressively covers a greater percentage of the filter-medium surface.

The data of Figures 3 to 11 on the media therefore show that the filtration cycle generally passes through a number of modes. In each case a portion of the cycle can be satisfactorily represented by the mode of standard blocking, while one or more regions appear to follow the mode of cake filtration even though a true cake does not exist in a macroscopic sense. Data for the region between the start of filtration and the region of standard blocking and between the region of standard blocking and that of cake filtration seem to represent transition zones. Attempts to apply the complete-blocking law (Table 1) to the initial region of filtration period failed in each case,

arithmetic plots of q_w vs. V_w resulting in smooth curves. It was found, however, that logarithmic plots of both q_w vs. V_w and q_w vs. t did give a straight line for this initial region (Figure 12). Consideration of this showed that as a result a simple logarithmic plot of V_w vs. t would be a straight line. This was verified for each medium (Figure 13) over this initial region of filtration. The resulting empirical relationship, $V_w = k't^m$, is not in agreement with any of the proposed filtration laws (Table 1). The value of m was very nearly 1.0 for four of the media and was near 0.7 for the other five examined. Vosters (*22*) has recently reported that filtration data for this initial region of filtration with viscose yield straight lines when plotted as log t vs. log t/V_w and has suggested an empirical relationship of the form $t/V_w = (t^{m''+1})/k''$. In general the data over the initial regions of filtration also correlate well by means of the method of Vosters. However, the direct exponential relationship between t and V_w appears to fit the data as well or better and is of a simpler form. Behavior during this initial period of filtration may be governed by the rapid change in the degree of particle retention occurring during this period. All the proposed filtration laws (Table 1) assume that the volume or number of particles removed per volume filtered remains constant. As this is far from true for this initial period of filtration even with very tight media, it is not surprising that all relationships of Table 1 fail for this period. Insufficient data were obtained over this period to describe adequately the rate of change of particle retention with volume filtered. Such data if taken into account in the derivation of the standard-blocking law may well result in a form similar to the empirical expression obtained. Attempts to apply the law of intermediate blocking to the transition region between standard blocking and cake filtration on the curves of Figures 3 to 11 were not successful. This region of filtration was of short duration in most cases and appears to be a true transition zone not amenable to any single relationship.

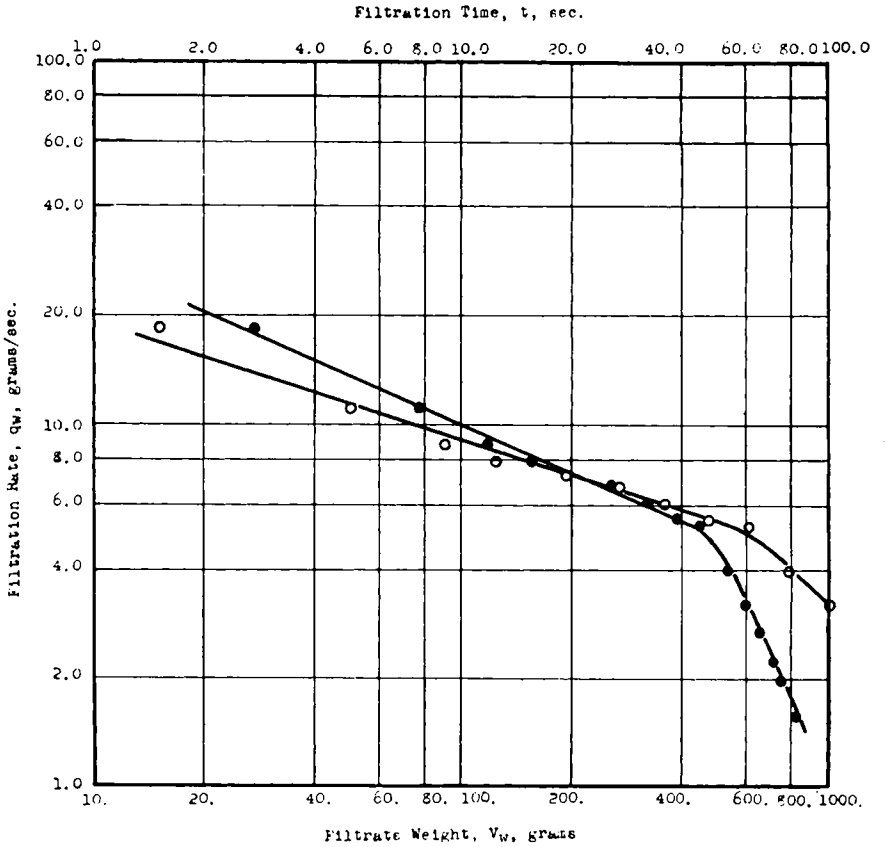

Fig. 12. Initial portion of clarification run FE-420 Orlon satin: ● q_w vs. V_w. ○ q_w vs. t.

Comparative Performance of Various Media

Plugging Characteristics. The comparative plugging rates of the various media can be judged best on the basis of the period of standard blocking. For this period the comparative slopes of the t/V_w vs. t curves (or the plugging constant K_s), as shown in Table 2, indicate directly the plugging rates expressed as the ratio of the packed volume of solids removed per gram of filtrate to the clogging value of pores within the filter medium. These values of K_s are all for very nearly the same conditions of pressure drop, solution viscosity, and initial solids concentration, as indicated in Table 2. The plugging constant K_s varied over a hundredfold range with the media examined, the value for Albany 220 felt being lowest, values for No. 8 cotton duck and TF-5071 being highest, and values for all others falling near the midpoint of these extremes. Although K_s is widely recognized as indicating the rate of plugging during the standard-blocking period, the present data indicate that K_s is also directly related to the volume of suspension which can be filtered through a medium before the end of the standard-blocking period is reached. Thus in Figure 14 a logarithmic plot of V_w/A at the end of standard-blocking period vs. $2/K_s$ results in a good approximation of a straight line. This indicates that capacity of a medium to the end of the standard-blocking period, V_w/A, is empirically related to K_s by

$$V_w/A = C\left(\frac{1}{K_s}\right)^{m''} \qquad (10)$$

at least for the system and conditions involved. This is of considerable significance, as filter media of widely different characteristics are involved. Thus it appears that K_s not only characterizes the rate of plugging of a medium for the standard-blocking period, but also the filtrate capacity of the medium before plugging, irrespective of the construction of the medium or the amount of bleed that occurs.

The straight-line intercepts obtained by extrapolation of the standard-blocking periods of Figures 3 to 11 to $t = 0$ also appear to bear a distinct relationship to the properties of the medium, despite the fact that the standard-blocking period is preceded by an initial period of filtration which establishes the actual $t = 0$ intercept. Thus the logarithmic plot of the intercept value (as given in Table 2) vs. the liquid resistance of the medium R_w' (as given in Table 1 of Part I of this paper) shows that a definite relationship exists (Figure 15). The indicated exponent is, however, less than the value of 1.0 which would be expected if no complicating factors were involved.

Particle-retention Characteristics and Relationship to Pore Structure. All clarification runs were characterized by a progressive decrease in the number of particles passing through the filter medium, as shown by the particle-count curves of Figures 3 to 11 for the > 3-μ particles. A similar decrease in number of particles passed occurred for the 3 to 5, 5 to 10, 10 to 15 and > 15-μ size ranges.* In general, the percentage by number of the < 3-μ particles passing uncollected exceeded 50% with all the media for the initial period of filtration preceding the standard-blocking region. Over this region the number of < 3-μ particles in the filtrate dropped very rapidly, indicating

*These data may be obtained as document 4956 from the American Documentation Institute, Photoduplication Service, Library of Congress, Washington 25, D. C., for $1.25 for photoprints or 35-mm. microfilm.

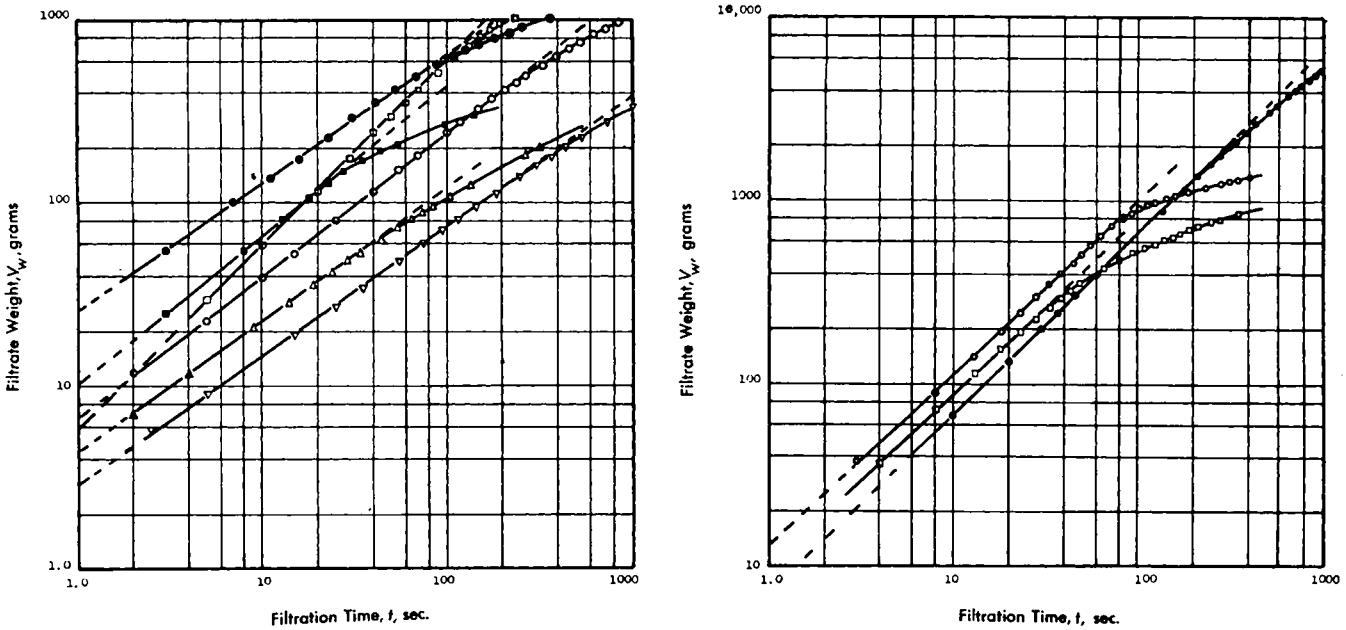

Fig. 13. (a) Initial portions of various clarification runs: ○ SN-23 staple nylon duck, ● FE-420 filament Orlon satin, □ 175-TW cotton twill, ■ TF-5044 filament nylon twill, △ TF-5071-F filament Orlon taffeta, calendered, ▽ No. 8 cotton duck; (b) initial portions of various clarification runs: ○ SN-7 filament nylon duck, ● AF-220 woven wool felt, □ TF-5071-U filament Orlon taffeta.

that during this initial region the large but relatively few interyarn or interthread pores became rapidly plugged to a degree which reduced their effective size to the same order of magnitude as the interfiber pores. At the start of the region of standard blocking, the percentage by number of < 3-μ particles passing uncollected ranged from 30 to 60% with the various media used. Similarly at the end of the region of standard blocking the percentage by number uncollected was from 10 to 30%. Over the observed regions of cake-law filtration with these media the percentage by number of < 3-μ particles uncollected was less than 10%.

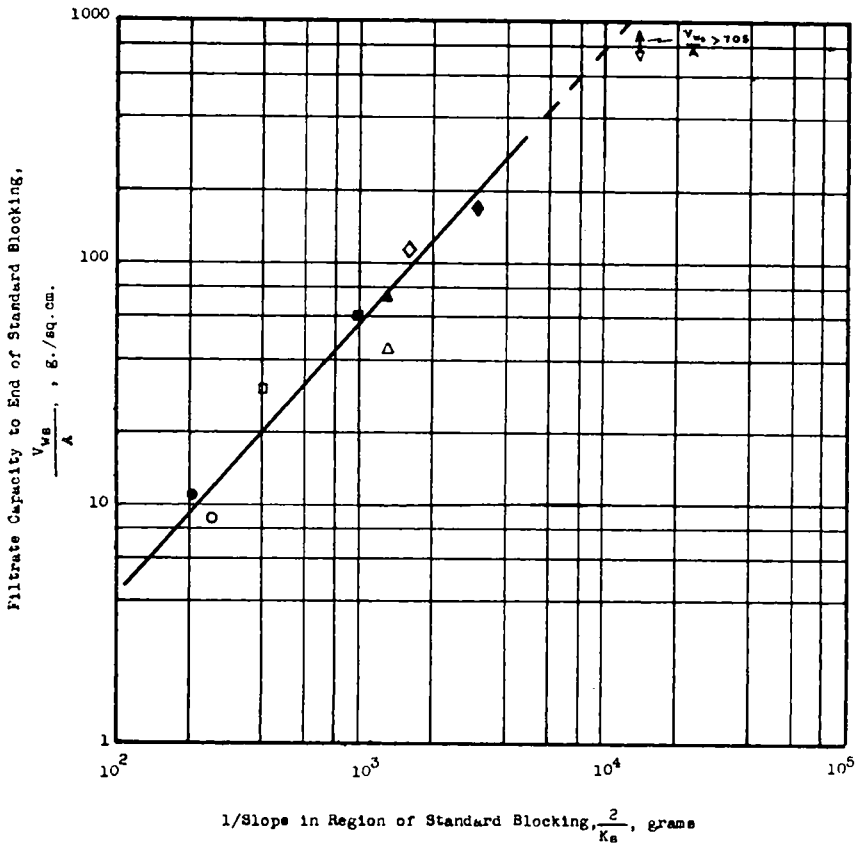

Fig. 14. Comparative capacity of various filter media to end of standard-blocking period: ○ No. 8 cotton duck, ● TF-5071-F, □ TF-5044, ■ TF-5071-U, △ SN-23, ▲ FE-420, ◇ SN-7, ◆ 175-TW, ▽ No. 220 felt.

As already discussed, at the solution viscosities and the filtration rates normally found in liquid filtrations, direct interception of particles from the streamlines of fluid adjacent to the pore walls is probably the major mechanism of collection. With this assumption the percentage of particles passing uncollected through a circular pore of radius r can be calculated on the basis that the particles are randomly distributed in the flowing liquid stream and that all within a distance of one particle radius of the wall will be collected. Since the < 3-μ particles as counted were all in the range of 1 to 3 μ diam., an average radius of 1 μ can be taken as representative of this fraction. If this particle radius, collection by the mechanisms of direct interception, and complete particle retention once collection occurs are assumed, the percentage of particles by number uncollected after passage through pores of various sizes would be as shown in the accompanying table:

Pore radius, μ	Predicted % < 3-μ particles uncollected
6.0	69.5
5.0	64
4.0	56.2
3.0	44.5
2.0	25
1.5	11.1

Since the modal values of the interfiber-pore radius for all but one of the media used were in the range of 2.2 to 5.3 μ, the observed values of 30 to 60% of < 3-μ particles passing uncollected at the start of the region of standard blocking agree well with these predicted values. This suggests that the standard-blocking region represents a region during which plugging of the interfiber pores is controlling and that the assumption of particle collection by direct interception is reasonably valid under these conditions. The passage uncollected during the standard-blocking region of a few particles of size equal to or greater than twice the modal value of interfiber-pore radius may reflect the actual distribution of interfiber-pore size or may result from the effective size of the plugged interyarn pores being greater than the interfiber pores.

Recently Cranston (*2*) developed a method whereby it should be possible at any instant in the filtration cycle to calculate the effective pore-size distribution of the medium if the particle-size distributions in both feed and filtrate are known at the same instant in the filtration cycle. The method has not actually been applied, however, because of the accurate particle-size-distribution data needed in the range of 0 to 5 μ for any worth-while calculations and because of the limited

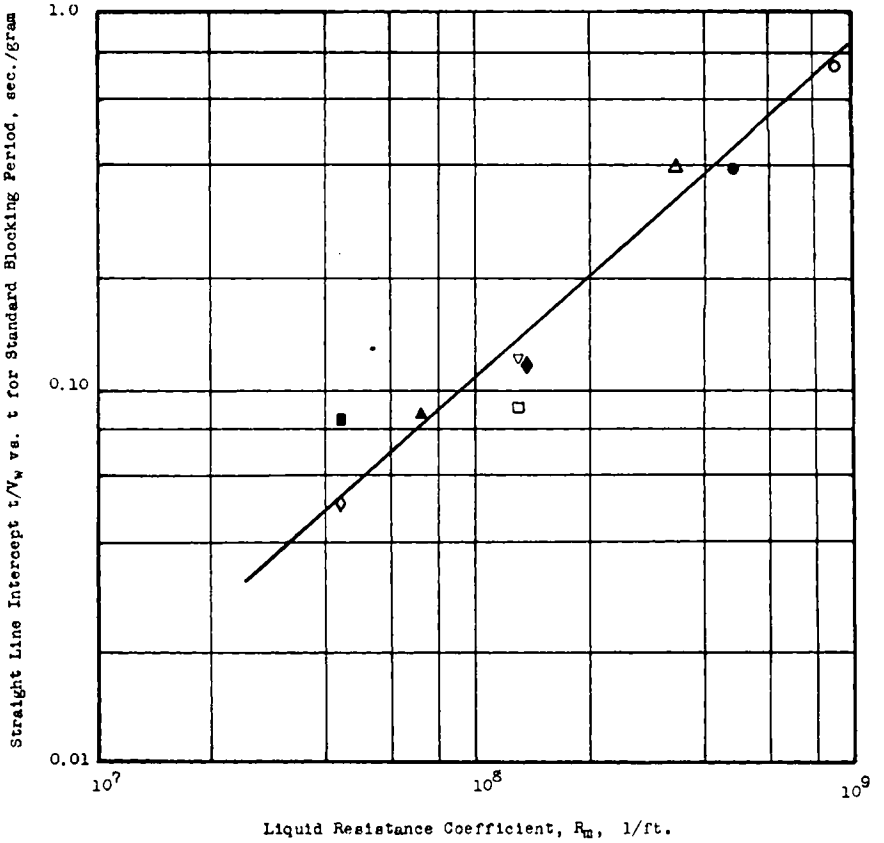

Fig. 15. Correlation of initial blocking resistance with liquid resistance of various filter media: ○ No. 8 cotton duck, ● TF-5071-F, □ TF-5044, ■ TF-5071-U, △ SN-23, ▲ FE-420, ◇ SN-7, ◆ 175-TW, ▽ 220 felt.

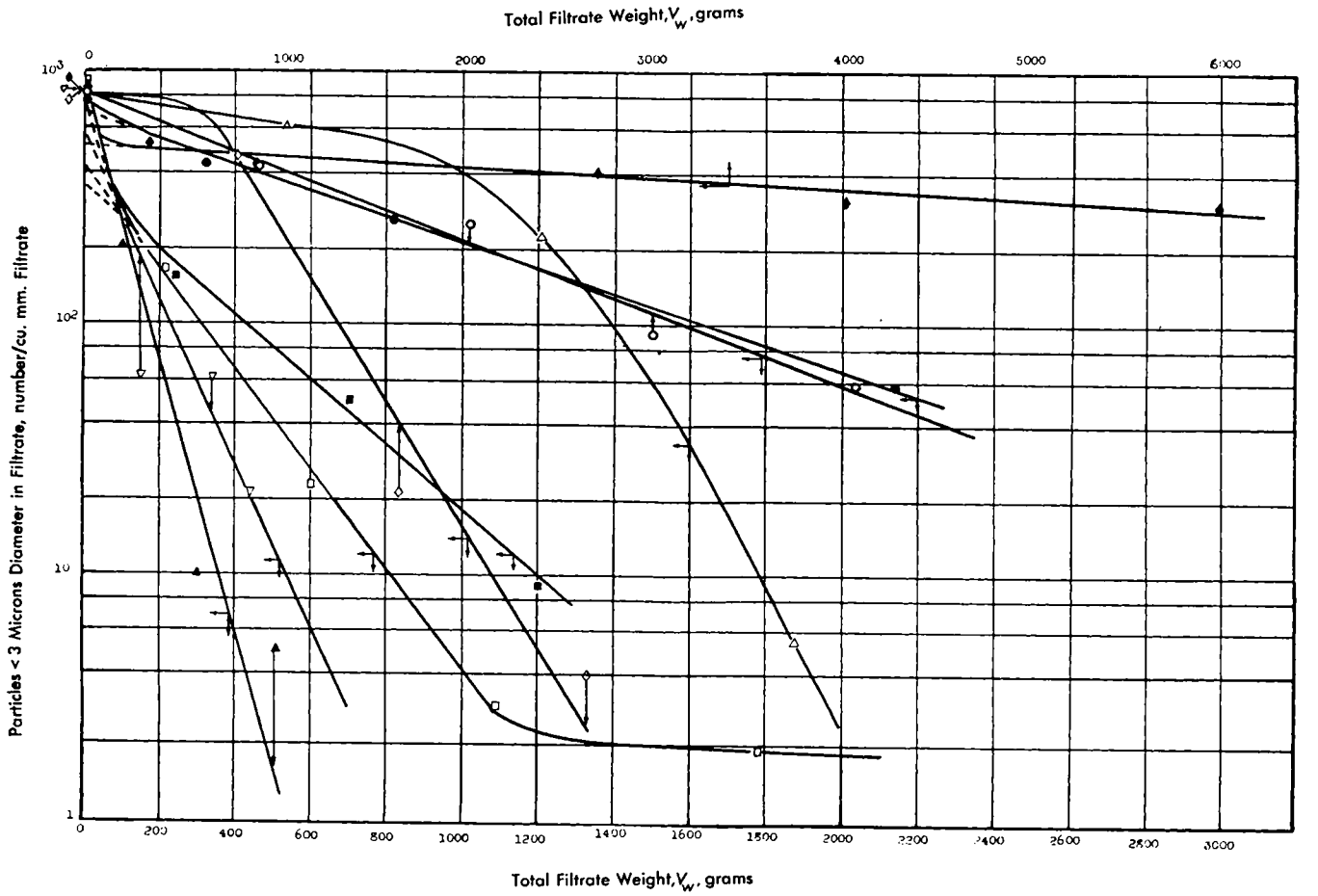

Fig. 16. Comparative particle-retention characteristics of various media: ○ 175-TW, ● FE-420, □ SN-23, ■ TF-5044, △ SN-7, ▲ No. 8 cotton duck, ◇ TF-5071-U, ◆ AF-220 felt, ▽ TF-5071-F.

utility of the results, as the effective pore-size distribution of the medium is changing continuously. The method, however, should also be applicable to the calculation of expected particle-size distribution in the filtrate at the start of a filtration provided that the particle-size distribution of feed and pore-size distribution of filter medium are known at the start of the filtration cycle. Since the mercury-intrusion method (Part I of the paper) provides an accurate pore-size distribution for a given medium, this reverse application of Cranston's method may have practical value but has not yet been applied to the data reported here. The particle-count data for < 3-μ particles passing uncollected with all media examined have been plotted vs. V_w on a semilogarithmic scale in Figure 16. For many of the media these plots approximate a straight line over most or all of the filtration cycle. This shows that the particle count in the filtrate decreases at a constant percentage rate throughout a significant portion of the filtration cycle. With the 175-TW cotton twill and the FE-420 satin medium made from Orlon acrylic fiber, this decrease in number continued at a constant percentage rate throughout the periods of initial blocking, standard blocking, and cake filtration. With very open cloths, such as 5071-U or SN-7, the percentage rate of decrease in particle number increased during the initial blocking period but remained constant throughout the standard-blocking and cake-filtration periods. With very tight cloths, such as No. 8 cotton duck, the percentage rate of decrease in particle number appeared to diminish during the initial blocking period but was constant throughout the remaining part of the filtration cycle. Thus, over the standard-blocking region and initial regions of cake-law filtration an empirical relationship of the form $C_0 = C_s e^{-BV}$ is indicated, where B is a constant which is related to the pore radius of the medium, C_s is the number of uncollected particles in the filtrate at the start of standard blocking,

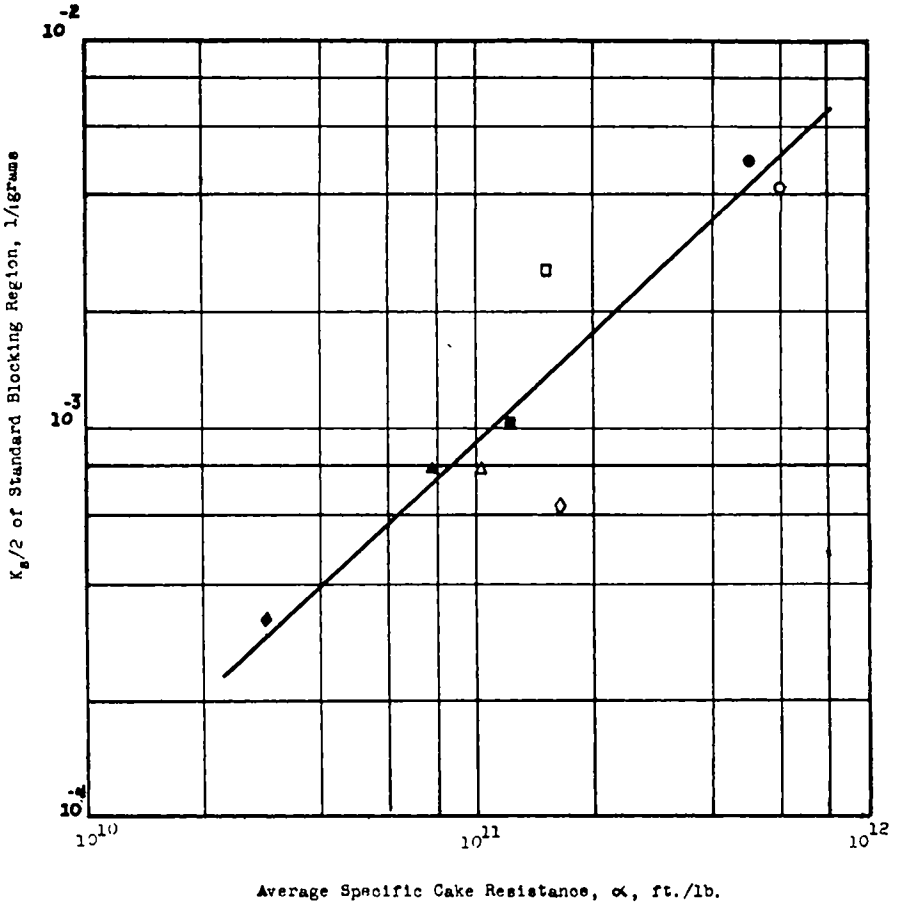

Fig. 17. Correlation between average specific cake resistance and standard-blocking performance: ○ No. 8 cotton duck, ● TF-5071-F, □ TF-5044, ■ TF-5071-U, △ SN-23, ▲ FE-420, ◇ SN-7, ◆ 175-TW.

and C_0 is the number of uncollected particles in the filtrate at any time after the start of standard blocking. At any point in a filtration cycle the over-all collection number N_c has been defined (*13* and *3*) by the relationship $C_0 = C_f e^{-N_c}$, where C_f is the number of particles in the feed. When written for the start of the standard-blocking region, this expression becomes $C_s = C_f e^{-N_c'}$, where N_c' is the over-all collection number at the start of standard-blocking filtration. Combining yields the general relationship $C_0 = C_f e^{-(N_c' + BV)}$ for constant-pressure filtration over the standard-blocking and initial cake-law periods of filtration.

Cake-filtration Characteristics. With all media except the AF-220 felt, one or more regions of cake-law filtration followed the region of standard blocking, as indicated by the straight-line portions of the t/V_w vs. V_w plots of Figures 3 to 11. In Table 2 are tabulated the values of the slope and intercept of the straight-line

TABLE 3. COMPARISON OF CLOGGING VALUES WITH TOTAL PORE VOLUME AND VOLUME OF FEED SOLIDS

	(1)	(2)	(3)	(4)	(5)	(6)	(7)
			Packed volume* of feed solids				
Filter-medium style	Total pore vol. of medium $AL\epsilon/A$, cc./sq.cm.	Clogging value of medium πNhr_0^2, cc./sq.cm.	To end of standard blocking period, cc./sq.cm.	To start of cake law filtration, cc./sq.cm.	Ratio, column (2)/ column (1)	Ratio, column (3)/ column (2)	Ratio, column (4)/ column (2)
175-TW Cotton twill	68×10^{-3}	8.3×10^{-3}	5.7×10^{-3}	6.4×10^{-3}	0.12	0.69	0.77
FE-420 Filament Orlon satin	18.6×10^{-3}	3.7×10^{-3}	2.7×10^{-3}	4.0×10^{-3}	0.20	0.73	1.08
SN-23 Staple nylon duck	46×10^{-3}	3.9×10^{-3}	2.2×10^{-3}	3.3×10^{-3}	0.085	0.57	0.85
TF-5044 Filament nylon twill	7.5×10^{-3}	1.2×10^{-3}	0.80×10^{-3}	1.3×10^{-3}	0.16	0.67	1.08
AF-220 Woven wool felt	220×10^{-3}	43×10^{-3}	18×10^{-3}	....	0.20	0.42	
TF-5071-0 Filament Orlon taffeta	43×10^{-3}	3.0×10^{-3}	2.4×10^{-3}	3.1×10^{-3}	0.070	0.80	1.03
SN-7 Filament nylon duck	21×10^{-3}	4.8×10^{-3}	4.0×10^{-2}	4.9×10^{-3}	0.23	0.83	1.02
TF-5071-F Filament Orlon taffeta, calendered	16×10^{-3}	0.63×10^{-3}	0.35×10^{-3}	0.67×10^{-3}	0.040	0.56	1.06
No. 8 Cotton duck	48×10^{-3}	0.73×10^{-3}	0.38×10^{-3}	1.1×10^{-3}	0.015	0.52	1.51

*Packing porosity of particles within pore, $\epsilon_p = 0.45$.

(cake-law) portions of these curves for the various media. With all media except the very tight No. 8 duck and TF-5071-F, the intercept obtained by extrapolation to $V_w = 0$ was negative. Such a negative intercept is obtained in normal cake filtrations only when initial bleed occurs. The curves of Figures 3 to 11 are extreme examples of this and show in detail how particle bleed and initial regions of blocking filtration shift the cake-filtration region, resulting in a reduced or negative

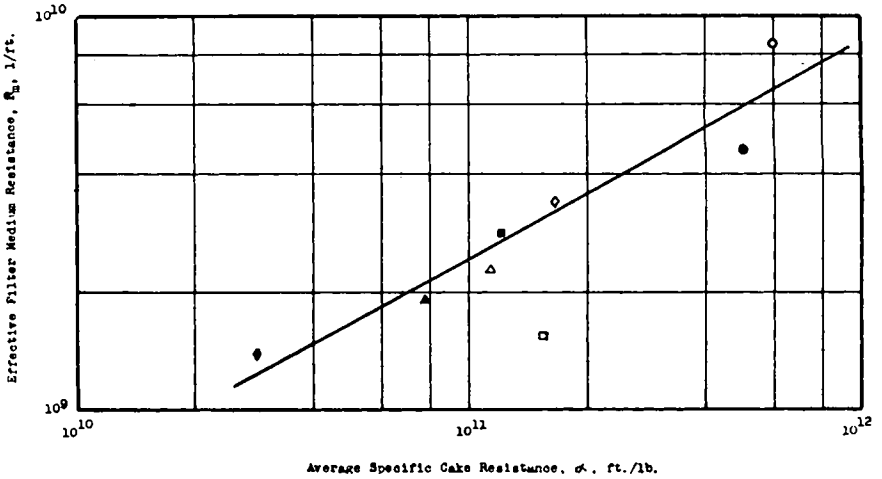

Fig. 18. Correlation of effective filter-medium resistance in cake filtration with average specific cake resistance: ○ No. 8 cotton duck, ● TF-5071-F, □ TF-5044, ■ TF-5071-U, △ SN-23, ▲ FE-420, ◇ SN-7, ◆ 175-TW.

intercept. In a qualitative sense the value of this extrapolated intercept is an indication of the amount of bleed which has occurred before cake filtration starts.

The values of α, corresponding to the regions of cake filtration for the various media, vary over a tenfold range (Table 2) despite the fact that the same well-dispersed suspension was used in each case. Also, with very tight media such as No. 8 cotton duck and TF-5071-F, two successive regions of cake filtration resulted, with the value of α decreasing for the second region. The absolute values of α are much higher than would be expected if they represented a true cake over the entire surface of the filter medium. Thus the value of α obtained by filtering a well-dispersed suspension of the same solids under identical filtration conditions except at a solids concentration of 6,100 p.p.m. by volume (48 g./liter) was constant at a value of $\alpha = 2.1\ (10)^{10}$ ft./lb., which was independent of the filter medium used. The values of α tabulated in Table 2 are two to thirty times this true value of α for a macroscopic cake. The photomicrographs of Figures 19 to 21 show the probable reason for this variation in the calculated value of α and for the high absolute values obtained. Thus, in general, no macroscopic cake was formed on the surface of the filter medium even at the end of the filtration cycle. Figures 19 to 21 show that only a microscopic cake had formed, both at each interyarn pore and at numerous isolated points on the surface of each yarn. Thus the effective filtration area at the cake surface was very much less than the surface area of the cloth. Also this effective surface area of the cake appears to vary for various media constructions during the regions of cake-law filtration involved. Since area enters as a squared term in the calculation of α, this lack of a macroscopic cake and variation in the points of forma-

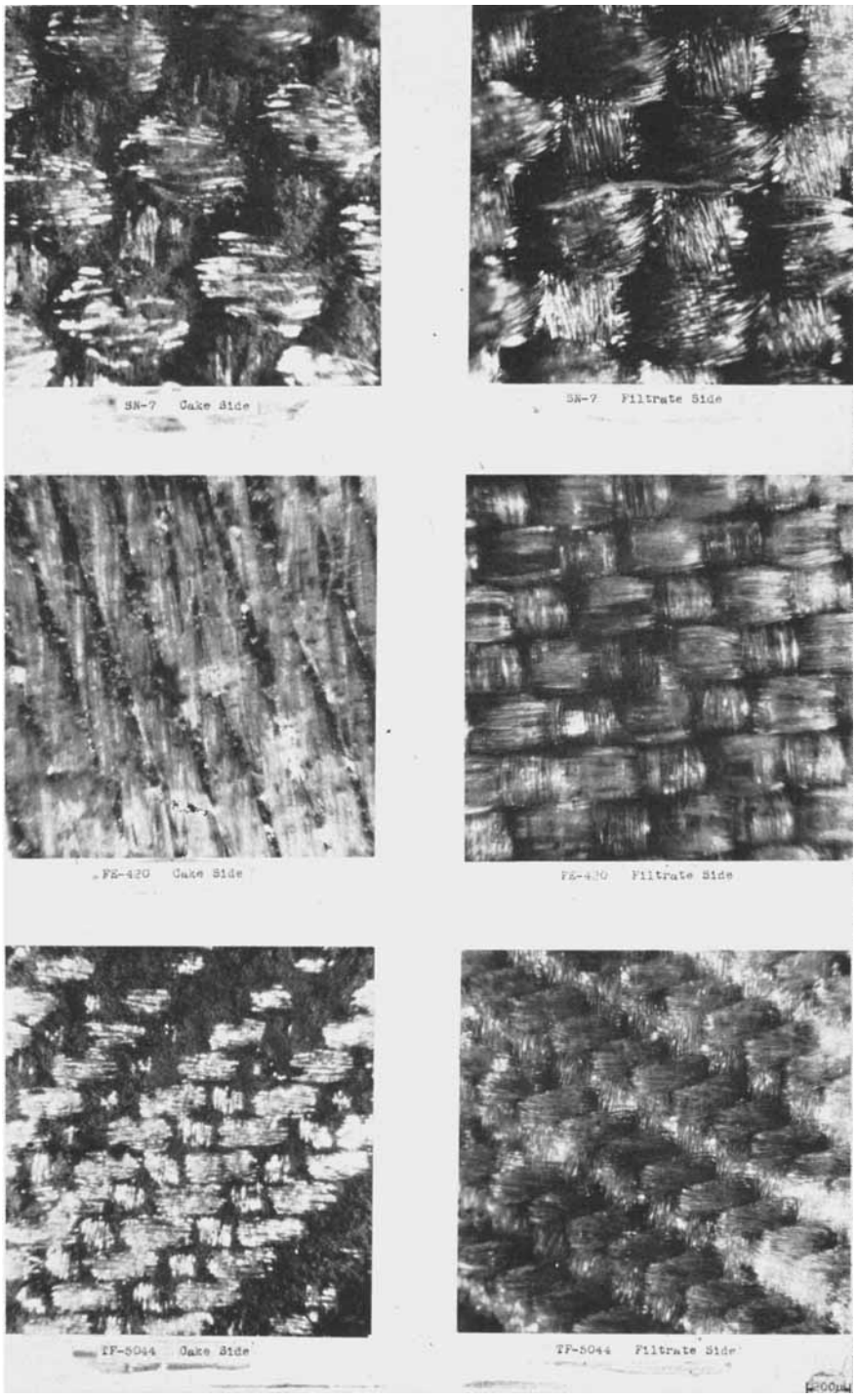

Fig. 19. Photomicrographs of filter-media surfaces at end of runs.

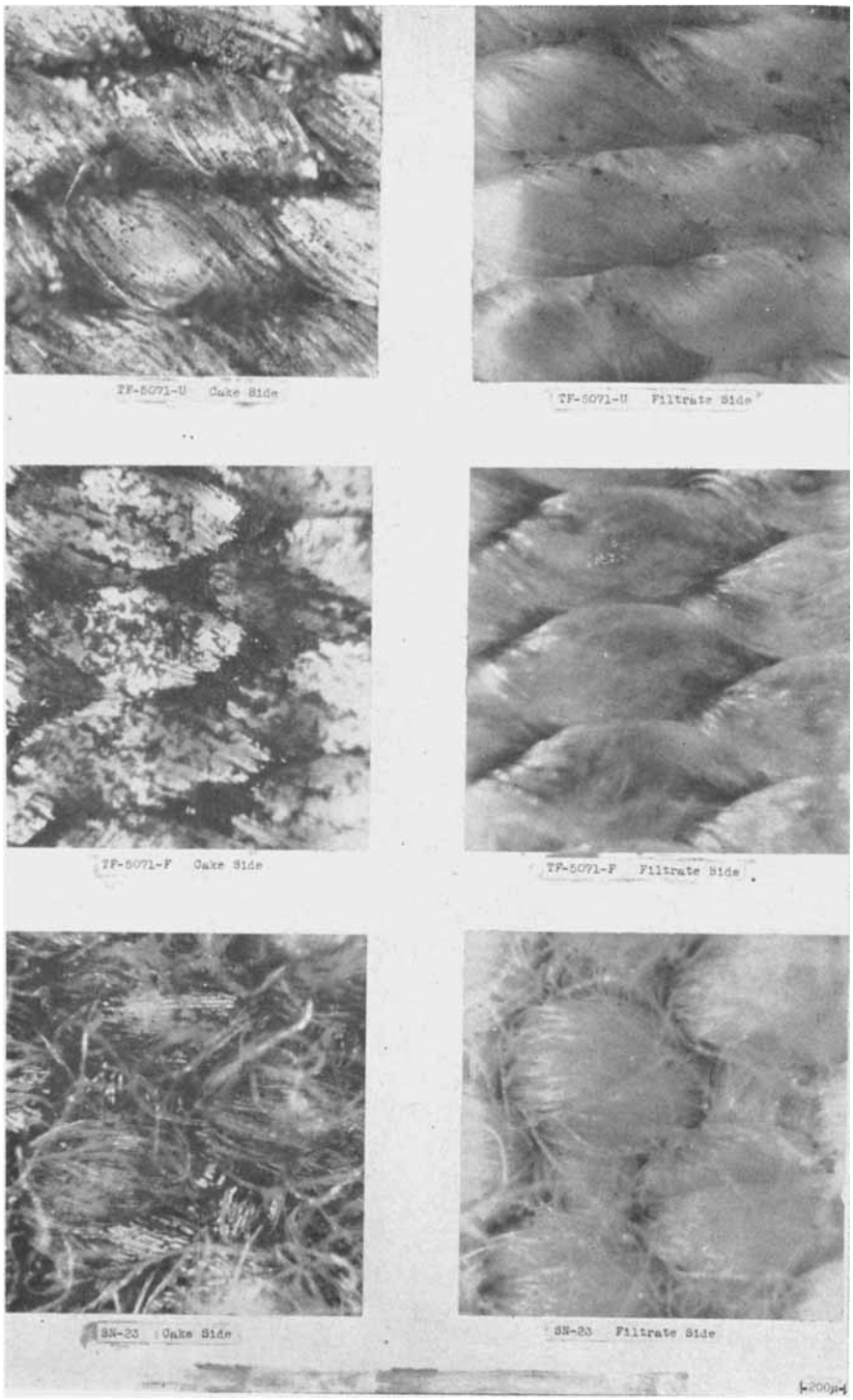

Fig. 20. Photomicrographs of filter-media surfaces at end of runs.

tion of the microscopic cake can easily account for the variability and the high absolute values of α. A changing cake-surface area during this period of cake filtration probably accounts for the successive regions of cake filtration encountered with the very tight media. This indicates that if the filtration cycle had been carried on until a macroscopic cake formed over the entire surface, a number of successive regions of cake filtration would result, with the values of α for successive regions decreasing to a final value which would be representative of a true macroscopic cake and thus independent of the filter medium. With rather loose cloths which tend to bleed particles even during the observed region of cake-law filtration, this particle bleed further complicates the picture. Thus final elimination of this bleed upon formation of a true macroscopic cake would have the opposite effect of tending to cause an increase in calculated α as a macroscopic cake forms.

In any case, Figures 19 to 21 show that the observed regions of cake-law filtration did not constitute true cake filtration with a macroscopic cake. These photomicrographs and the corresponding filtration data throw considerable light on how a cake forms on the surface of woven media. Despite the high yarn twist of the TF-5071-U and the TF-5071-F media, the photomicrographs of Figure 19 show that appreciable filtration is occurring through the yarn structure with cake formation at numerous isolated places on the surface of the yarn itself. In this respect, the photomicrographs show little difference between low and high yarn twist. However, the smaller interfiber pores resulting from both high-twist yarns and from calendering appear to minimize penetration of the yarns by particles and result in filtration with more rapid cake formation at the surface of the yarns.

The variability of the values of α obtained with various media appears to be closely related to the value of the plugging constant K_s obtained for the same medium during the standard blocking portion of the filtration cycle. Thus the plot of Figure 17 indicates an exponential relationship between $K_s/2$ and α. The apparent increase in observed α with increasing values of $K_s/2$ is related to the variation in the clogging value $\pi N h r_0^2$ from medium to medium, smaller clogging values causing higher values of plugging constant and a reduced area of pore constriction at which cake-law filtration starts. Thus the greater the plugging constant in these runs, the lower the true cake-forming area at the start of cake filtration and the greater the value of α computed for the initial region of cake-law filtration by use of the total filter-medium area. The effective resistance of the filter medium at the start of the region of cake-law filtration can be calculated from the instantaneous $\Delta t/\Delta V_w$ values at this point in the filtration cycle. Such values of R_m, as given in Table 2, appear unrelated to the liquid resistance of the unused medium. Rather, these values of R_m appear closely related to the value of α obtained from the region of cake-law filtration with each respective medium. This is shown by the logarithmic plot of Figure 18. With the more open media, the value of R_m was near a value equal numerically to 0.1α, which experience in true cake filtration (*6*) has shown to be the usual order of magnitude of R_m. However, as the media became tighter, the ratio of R_m/α decreased, with $R_m = 0.01\alpha$ for the very tight media. This low value of the R_m/α probably results from lack of a macroscopic cake in the observed region of cake-law filtration, which causes the calculated value of α to be too large.

Comparison of Filtration Performance with Pore Volume and Pore Size of the Filter Media. Clogging values $\pi N h r_0^2$ for the various filter media used are computed in Table 2 by use of Equation (8) and the slope of the corresponding t/V_w vs. t plot of the filtration data for the region of standard blocking. Based on previous measurements (*5*) a value of $\epsilon_p = 0.45$ was used for the packing porosity of the

particles retained on the pore walls. These clogging values represent the effective pore volume of the filter medium which plugs during this standard-blocking period of filtration. In Table 3 these clogging values are compared with the total pore volume of each filter medium. The clogging value of pore volume is seen to range from 1.5 to 23% of the total pore volume. The ratio of the clogging value to the total pore volume is smallest for the tightest media but otherwise seems independent of the construction of the filter medium. For media other than the tightly woven No. 8 cotton duck and 5071-F calendered Orlon the clogging value was from 7 to 23% of the total pore volume. This percentage of the pore volume can be interpreted to represent the volume of the pore constrictions which is controlling insofar as particle buildup and plugging are concerned.

Also shown in Table 3, for the various media, is a comparison of the clogging values with the total packed volume of solid particles fed to both the end of the standard-blocking region and the start of the region of cake-law filtration. The packed volume of the solids fed to the end of the standard-blocking region is seen to range from 52 to 83% of the clogging value of pore volume. The packed volume of the solids fed to the start of the region of cake-law filtration is seen to range from 77 to 151% of the clogging value of pore volume, with five of the media showing packed volume of feed solids to equal the clogging value $\pm 10\%$ at the start of cake-law filtration. These figures then support the interpretation of the clogging value as the volume of the pore constrictions which is controlling insofar as particle buildup and plugging are concerned. Failure of the standard-blocking relationship before 100% of the clogging value of pore volume is filled with packed particles, and the existence of a transition region between the regions of standard-blocking and cake-law filtration may result from at least two factors. First, as that portion of the pore volume represented by the clogging value becomes more than half filled with packed particles, an appreciable part of the flow may occur through the smaller pores between the packed particles along the pore wall, causing a combination of standard-blocking and cake-law filtration. Second, since the r_0 term of the clogging value, $\pi N h r_0^2$, is not a constant but rather a distribution of sizes, some of the pore constrictions representing the clogging value of pore volume may become plugged before others, resulting in cake-law filtration through some pore constrictions while filtration through other constrictions still follows the standard-blocking mode. This second factor can be expected to be more pronounced in constant-rate filtration than in constant-pressure filtration.

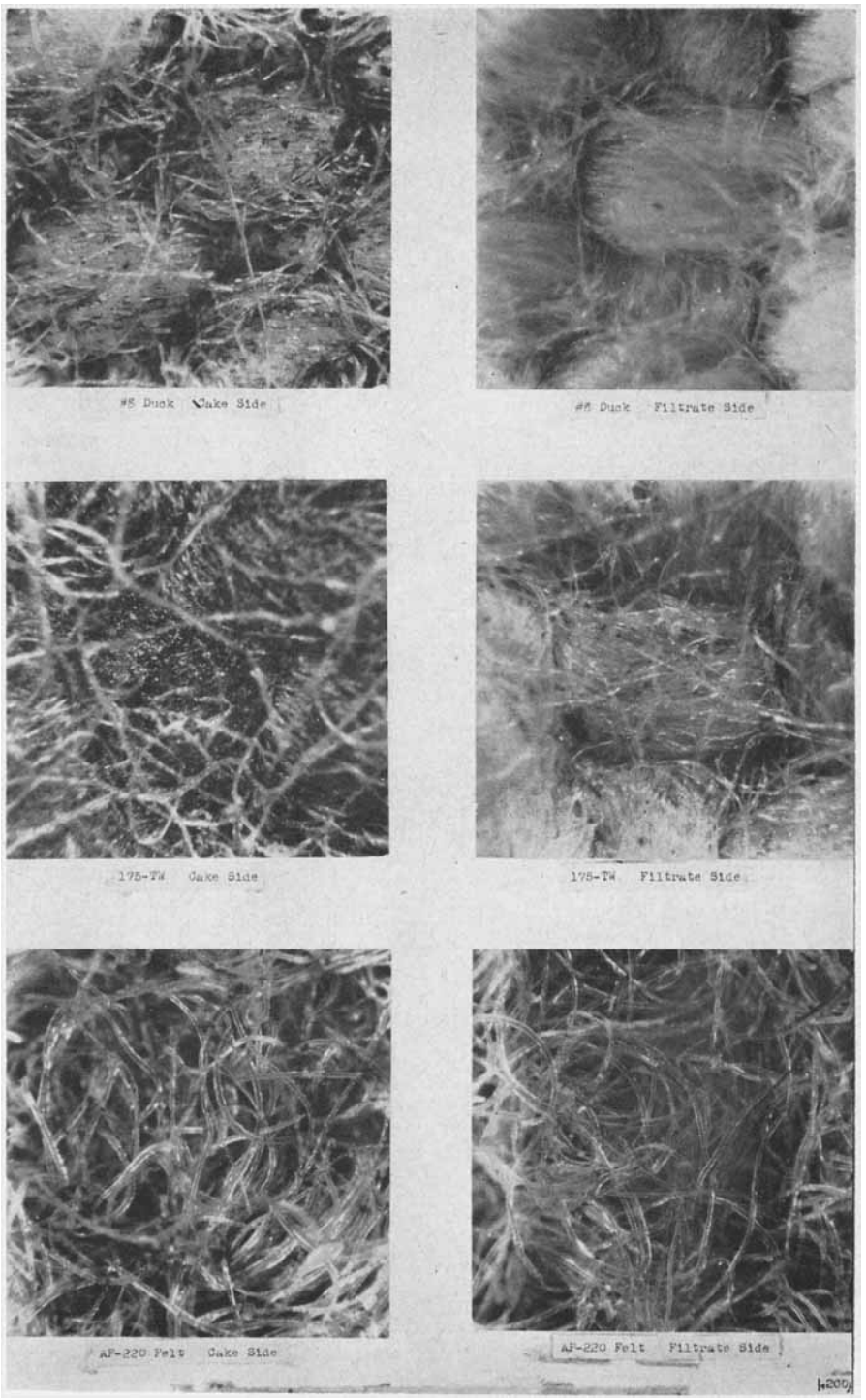

Fig. 21. Photomicrographs of filter-media surfaces at end of runs.

With the physical picture of buildup of packed particles on the walls of the pore constrictions represented by the clogging value of pore volume, a basic difference between constant-pressure and constant-rate filtration during the region of standard blocking becomes clear. Thus the shear stress at the walls of these constrictions is equal to either $r(\Delta p)/2h$ or $(\mu_f/g_c)\ (4q/\pi r^3)$, where $r = r_0$ at the start of standard-blocking filtration and r decreases as a packing of particles builds up on the walls. With flow through the packing of the particles neglected, the shear stress at the wall or surface of packed particles on the wall then decreases with constant-pressure filtration, but increases with constant-rate filtration. As already discussed, particle retention increased during the standard-blocking period of filtration for the constant-pressure filtrations reported here. Few data on particle retention for constant-rate filtration during the standard-blocking period have been reported, and it is not clear whether the degree of retention actually decreases short of breakthrough. The fact that particle collection by interception will tend to increase as the radius term of the clog-

Table 4. Analysis of Clogging Values in Terms of Circular Pores of Measured Interfiber Pore Radius

Filter-medium style	Filter-medium porosity, ϵ void fraction	Modal value of interfiber pore radius, r_f, cm.	Calculated values assuming $r_0 = r_f$: hN, 1/cm.	$\pi hN/b$,* cm.	Constriction-free area/ avg. pore-free area a, dimensionless	Population density of plugging pores, N, No./sq. cm.	Effective length of plugging pores, h, cm.	Ratio of h/L, dimensionless
175-TW Cotton twill	0.603	5.3×10^{-4}	9.5×10^{3}	6.3×10^{-4}	0.35	2.4×10^{5}	4.0×10^{-2}	0.36
FE-420 Filament Orlon satin	0.517	3.9×10^{-4}	7.8×10^{3}	5.2×10^{-4}	0.44	4.7×10^{5}	1.6×10^{-2}	0.46
SN-23 Staple nylon duck	0.505	4.0×10^{-4}	7.8×10^{3}	5.2×10^{-4}	0.23	2.3×10^{5}	3.4×10^{-2}	0.38
TF-5044 Filament nylon twill	0.413	3.0×10^{-4}	4.2×10^{3}	2.8×10^{-4}	0.37	5.5×10^{5}	0.79×10^{-2}	0.44
AF-220 Wool felt	0.701	16.5×10^{-4}	5.0×10^{3}	3.4×10^{-4}	0.22	0.18×10^{5}	27.6×10^{-2}	0.91
TF-5071-U Filament Orlon taffeta	0.528	3.8×10^{-4}	6.6×10^{3}	4.4×10^{-4}	0.38	4.5×10^{5}	1.5×10^{-2}	0.18
SN-7 Filament nylon duck	0.523	5.0×10^{-4}	6.2×10^{3}	4.1×10^{-4}	0.47	3.1×10^{5}	1.9×10^{-2}	0.49
TF-5071-F Filament Orlon taffeta, calendered	0.296	2.2×10^{-4}	4.1×10^{3}	2.7×10^{-4}	0.22	4.3×10^{5}	0.97×10^{-2}	0.18
No. 8 Cotton duck	0.537	2.9×10^{-4}	2.8×10^{3}	1.9×10^{-4}	0.073	1.5×10^{5}	1.9×10^{-2}	0.21

$$hN = \frac{\text{(measured clogging value)}}{\pi r_0^2} \qquad h = \frac{\text{(measured clogging value)}}{a\epsilon} = \frac{\text{(measured pore resistance)}(\pi N r_0^4)}{8}$$

$$N = \frac{a\epsilon}{\pi r_0^2} \qquad a = \left(\frac{1}{\epsilon r_0}\right)\sqrt{\frac{(8)\ \text{measured clogging value}}{\text{measured pore resistance}}}$$

*$b = 4.7(10)^7$, determined from empirical correlation of Figure 22a

ging value decreases complicates the picture for the case of constant-rate filtration.

In Figure 22a is shown a logarithmic plot of the clogging, πNhr_0^2, vs. the modal value of interfiber pore radius, r_f, for the various media as determined by the mercury-intrusion method. A good correlation is indicated of the form

$$\pi Nhr_0^2 = br_f^n \qquad (11)$$

in which $n = 3.0$ and $b = 4.7(10)^7$ cm^{-2}. This is strong evidence of a definite relationship between the radius, r_0, of the pore constrictions at which plugging occurs and the measured value of interfiber pore radius, r_f. Further, the value of $n = 3.0$ suggest that the value of the product Nh may vary in direct proportion to the value of r_0, which would result in a direct relationship between r_0 and r_f. The fact that the particle retention, calculated on the basis of r_f and the assumed mechanism of collection by interception, is in the range of observed particle retention lends support to this hypothesis. When it is recognized that measurements by the mercury-intrusion method result in the distribution of pore size in terms of the pore volume which can be entered through constrictions of a certain size, the equality of r_f and r_0 appears to be a reasonable approximation.

The plotting of the clogging value vs. the average pore radius, as measured by the permeability method (Figure 22b), shows that a relationship similar to that of Figure 22a appears to exist. The slope is again 3 although the scatter of data is greater. However, this relationship is believed to be a secondary one which results from the primary relationship of Figure 22a and a direct relationship between the values of r_f measured by the mercury-intrusion method and the values of r_p measured by the permeability method. The fact that particle retention calculated on the basis of r_p is very much less than the observed values indicates that r_p and r_0 cannot be equivalent. Consideration of the permeability method of measuring r_p also indicates that r_p would be expected to be considerably larger than the pore constrictions and therefore not equivalent to r_0.

If r_f is assumed equivalent to r_0, values of the pore-population density, N, and effective pore length, h, can be calculated from the measured values of the clogging value, πNhr_0^2, and pore resistance, $8h/\pi Nr_0^4$, as discussed in the Appendix. In order to give additional meaning to this for an actual filter medium which has pores containing constrictions of radius r_0 rather than straight-through pores of uniform radius, use is made of the relationship

$$N = a\epsilon/\pi r_0^2 \qquad (12)$$

in which ϵ is the measured value of the average porosity of the medium, and a

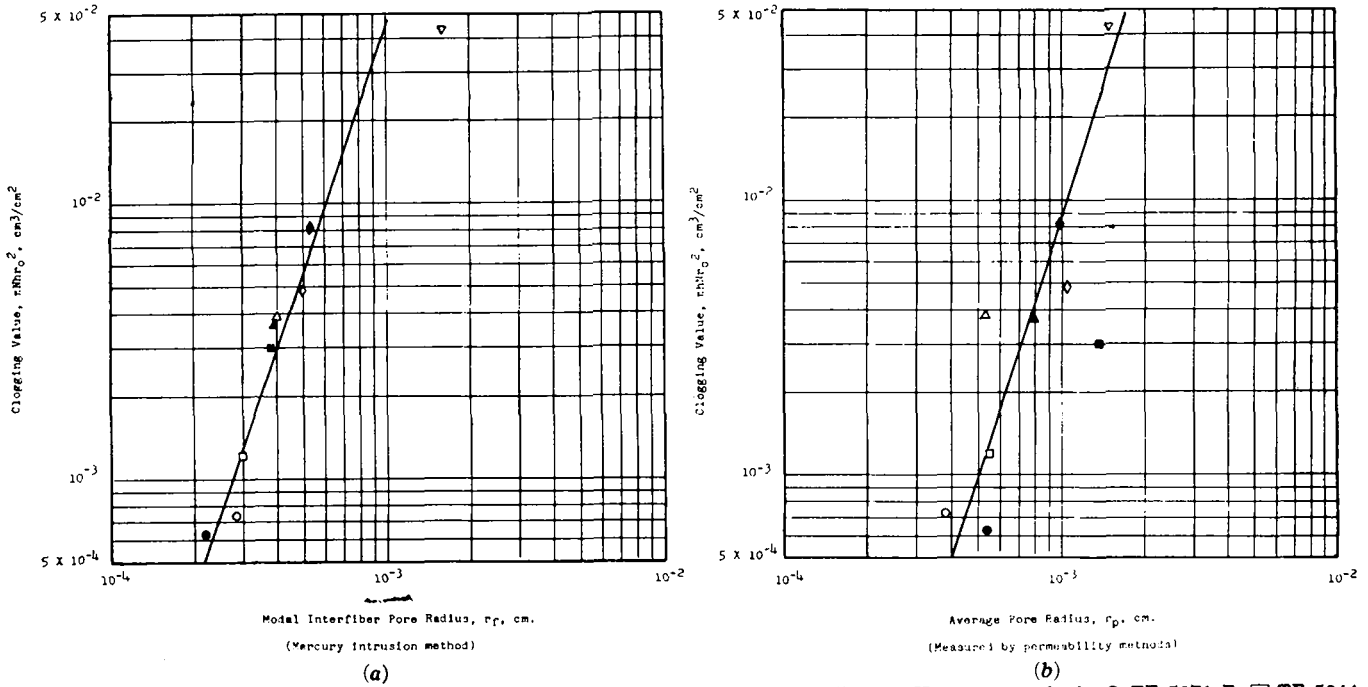

Fig. 22. (a) Correlation of clogging values with measured values of interfiber pore radius: ○ No. 8 cotton duck, ● TF-5071-F, □ TF-5044, ■ TF-5071-U, △ SN-23, ▲ FE-420, ◇ SN-7, ◆ 175-TW, ▽ 220 felt; (b) correlation of clogging values with measured average pore radius: ○ No. 8 cotton duck, ● TF-5071-F, □ TF-5044, ■ TF-5071-U, △ SN-23, ▲ FE-420, ◇ SN-7, ◆ 175-TW, ▽ 220 felt.

is the fraction of average cross-sectional area of the pores existing at the constriction of radius r_0. Thus, a can be thought of as the minimum free area represented by the constrictions of radius r_0 which become plugged during filtration. The values of N, h, and a, calculated on the assumption that $r_0 = r_f$, are given in Table 4. As expected, the values of the product hN are approximately proportional to the values of r_0. The scatter can be seen by comparing r_f numerically to the quantity $\pi hN/b$. Only the values for the AF-220 felt disagree badly, indicating that the assumption of $r_f = r_0$ is probably valid except for the felt. Permeability measurement of average pore size on this felt, as reported in Part I, showed that, because of swelling in aqueous solution, the pore size in this medium decreased markedly when water wet. Since the measured value of r_f was determined on the dry felt, while the solution filtered contained 20% water, it is not surprising that the measured value of r_f is indicated to be too large to fit the correlation.

The calculated values (Table 4) of a, the ratio of free area of pore constrictions to average free area of pores, ranged from 0.07 to 0.44 with the various media. This suggests that the radius, r_0, at the pore constrictions was in the range of 27 to 66% of the average radius of the pores. The ratios of the effective pore length, h, to the measured thickness of the medium (Table 4) was less than 1.0 in all cases and fell in the range of 0.18 to 0.44 for all media except the felt. The examination of many more media appears necessary before the real meaning of the calculated values of h, a, and N can be established; however, the values obtained for the media studied here appear consistent with the physical picture of medium structure and particle removal by the plugging of pore constrictions, as already discussed.

The empirical relationship of Figure 22*a* and Equation (11) may be of great practical significance. Since the values of interfiber pore radius and clogging values on which this relationship is based cover media of widely different construction, prediction of clogging values for other media should be possible based on measurement of pore-size distribution. Consideration of the nature of the clogging value leads to the conclusion that this value is a property of the filter medium which can be expected within limits to be independent of the concentration or size distribution of the particles in the feed suspension. Thus the variation in the over-all plugging constant, K_s, with such changes in feed suspension may in fact result only from variations in the numerator, $c/(1 - \epsilon_p)$, of the second term of Equation (9). If this can be verified, prediction of the changes in over-all plugging constant resulting from changes in feed suspension with a given medium will follow. The problem of predicting filtration performance from either measured or predicted clogging values is greatly complicated, however, if the filter medium is either compressible within the range of operating pressures to be encountered or is physically changed by absorption of the liquid being filtered. Either of these factors can greatly alter the clogging value of the medium, and these effects were purposely minimized by the conditions used in the work reported here.

SUMMARY

The application of a clarification technique to the evaluation of the performance of nine widely different filter media of previously determined pore structure has shown the following observations.

1. A region of standard-blocking filtration occurs with each medium, and thus a characteristic clogging value which is a measure of the volume of pore constrictions that plug during filtration can be determined.

2. The region of standard-blocking filtration ends when 50 to 80% of the clogging value of pore volume becomes filled with packed solids.

3. An initial region of cake-law filtration begins when the packed volume of solids removed becomes 80 to 150% of the clogging value of pore volume.

4. This initial region of cake-law filtration represents cake filtration on a microscopic rather than a macroscopic scale, such that the specific cake resistance computed on the basis of the superficial filtration area is two to thirty times the actual specific cake resistance and is dependent on the pore structure of the filter medium.

5. The degree of particle removal during the region of standard-blocking filtration is of the same magnitude as that calculated on the basis of particle removal by direct interception at the walls of pore constrictions of radius equal to the modal value of interfiber-pore radius.

6. A definite correlation exists between the clogging value, measured for the region of standard-blocking filtration, and the modal value of interfiber-pore radius of the medium.

7. This correlation strongly suggests equality between the radius of pore constrictions which plug during standard-blocking filtration and the modal value of interfiber-pore radius as measured by the mercury-intrusion method.

8. The work directed along the lines

nitiated here may ultimately make possible prediction of filter-media performance on the basis of pore structure, but the limitations imposed by variables not considered here must first be evaluated.

NOTATION

a = fraction of average free area of pores existing as plugging restrictions, dimensionless
A = superficial filtration area at surface of filter medium or cake deposited thereon, sq. cm.
b = constant in empirical relationship, 1/sq. cm.
B = exponent in empirical equation $C_0 = C_s e^{-BV}$, dimensionless
c = volume of solid particles removed per volume of solution filtered, cc./cc.
c_f = volume of solid particles in feed suspension per volume of solution, cc./cc.
C = constant in empirical equation, 1/sq. cm.
C_f = number of particles per unit volume of feed suspension, 1/cc.
C_0 = number of particles per unit volume of filtrate at any time, 1/cc.
C_s = number of particles per unit volume of filtrate at start of standard-blocking region, 1/cc.
g_c = conversion factor in Newton's law of motion, 980 (g.) (cm.)/(g. force)(sec.)^2
h = pore length in standard-blocking equation, cm.
k = constant in general differential equation for filtration cycle (dimensions depend on value of exponent, n)
k', k'' = constants in empirical equation for initial portion of filtration cycle
K = constant of Kozeny-Carman relationship ($5 \pm 10\%$), dimensionless
K_b = plugging constant of complete-blocking law, 1/sec.
K_s = plugging constant of standard-blocking law, 1/cc. (1/g. when V_w is used)
K_i = plugging constant of intermediate-blocking law, 1/cc. (1/g. when V_w is used)
K_c = plugging constant of cake-filtration law, sec./cm.^{6} (sec./g.^{2} when V_w is used)
L = measured thickness of filter medium, cm.
m, m', m'' = exponents of empirical relationships
n = exponent of general differential equation for filtration process
N = number of pores per unit area, number/sq. cm.
N_c = collection number as defined by equation $C_0 = C_f e^{-N_c}$, dimensionless
N_c' = collection number at start of standard-blocking region, dimensionless
Δp = total pressure drop (across filter medium and cake if any) at time, t, during filtration, lb./sq. in.
Δp_0 = total pressure drop at start of filtration, lb./sq. in.
q = filtration rate at time, t, during filtration, cc./sec. (g./sec. when V_w is used)
q_0 = filtration rate at start of filtration, cc./sec. (g./sec. when V_w is used)
q_w = rate of liquid passage through unused filter medium in permeability measurements in viscous flow range, cc./sec.
r = effective pore radius in medium at any time, t, during filtration, μ
r_f = modal value of interfiber-pore radius as measured by mercury intrusion method, μ
r_0 = effective initial pore radius in standard-blocking equation, cm.
r_p = average pore radius of filter medium calculated from liquid permeability measurements, μ
R_m = effective resistance of filter medium during cake filtration, 1/ft.
t = time of filtration, sec.
V = cumulative volume of filtrate at time, t, cc.
V_w = cumulative weight of filtrate at time, t, g.
w = weight of suspended solids per unit volume of filtrate, lb./cu. ft.
α = average specific cake resistance, ft./lb.
ϵ = porosity of filter medium, void fraction, dimensionless
ϵ_p = packing porosity of particles deposited on pore walls, void fraction, dimensionless
ρ_f = density of solution, fluid, or filtrate, g./cc.
ρ_s = density of suspended solid, g./cc.
μ_f = viscosity of solution or filtrate, centipoises

LITERATURE CITED

1. Carman, P. C., *Trans. Inst. Chem. Engrs. (London)*, **16**, 168 (1938).
2. Cranston, R. W., *Aircraft Eng. (London)*, **24**, 154 (1952).
3. Davies, C. N., *Arhiv. Hi. Rada*, **1**, 4 (1950); *Proc. Inst. Mech. Engrs. (London)*, **1B**, 185 (1952).
4. Gonsalves, V. E., *Rec. trav. chim.*, **69**, 873 (1950).
5. Grace, H. P., *Chem. Eng. Progr.*, **49**, 303 (1953).
6. *Ibid.*, 367 (1953).
7. Heertjes, P. M., and H. v. d. Haas, *Rec. trav. chim.*, **68**, 361 (1949).
8. Hermans, P. H., and H. L. Bredée, *Rec. trav. chim.*, **54**, 680 (1935); *J. Soc. Chem. Ind.*, **55T**, 1 (1936.)
9. Herrent, P., A. Lunde, and G. Jnoff, *Svensk Papperstidn.* **54**, 153 (1951).
10. Hixson, A. W., L. T. Work, and I. H. Odell, *Trans. Am. Inst. Mining Met. Engrs.*, **73**, 225 (1927).
11. Kane, E. D., *Ind. Eng. Chem.*, **45**, 860 (1953).
12. Kohl, J., and R. D. Zentner, *J. Phys. Chem.*, **57**, 68 (1953).
13. Langmuir, I., "Smokes and Filters," No. 865, Part IV, U. S. Off. Sci. Res. & Dev. (1942).
14. Matthes, A. von, *Chem. Tech.*, **3**, 13 (1951).
15. Nicolaysen, V. B., and W. B. Borregard, *Norsk Skogind.*, **4**, 219 (1950), **6**, 338 (1952).
16. Rodebush, W. H., "Handbook on Aerosols," Chap. 9, U. S. Atomic Energy Commission, Washington, D. C. (1950).
17. Ruth, B. F., *Ind. Eng. Chem.*, **27**, 806 (1935).
18. Samuelson, O., *Svensk Papperstidn.*, **52**, 465 (1949).
19. Smith, E. G., *Chem. Eng. Progr.*, **47**, 545 (1951).
20. Thomas, D. J., *Inst. Heating Ventilating Engrs. (London)*, **20**, 35 (1952).
21. Vosters, H., *Svensk Papperstidn.*, **53**, 29, 613, 771 (1950).
22. *Ibid.*, **54**, 539 (1951).

APPENDIX

Modified Development of Standard-Blocking Relationships

The physical picture assumed in deriving the standard-blocking law of Hermans and Bredée is that the filter medium consists of parallel pores of equal length and radius. The mechanism assumed is one of direct interception of particles from streamlines adjacent to the pore walls and of particle retention on the walls of the pores in such a way that the volume of the major flow channel through the pores decreases in direct proportion to the volume of filtrate which passes through the pore. This means that for standard blocking to occur over a period of considerable duration, the initial pore diameter of the medium must be at least several times the particle diameter even at very low solids concentration.

In a capillary of round cross section of radius r_0 and length h, through which passes a volume of liquid, dV, from which is removed a volume, c, of filterable particles per unit volume of liquid filtered, the reduction in volume of the original capillary channel will equal the packed volume of solids deposited, or

$$-2\pi NAhr\,dr = \left(\frac{c}{1-\epsilon_p}\right) dV \quad \text{(A1)}$$

where ϵ_p is the porosity of the layer of retained particles. Integrating between the limits of the start of filtration and the point where the volume filtered is V and the radius is r gives

$$-2\pi NAh \int_{r_0}^{r} r\,dr = \frac{c}{1-\epsilon_p} \int_0^V dV \quad \text{(A2)}$$

$$\pi NAh(r_0^2 - r^2) = cV/(1-\epsilon_p) \quad \text{(A3)}$$

From Poiseuille's law, the instantaneous time rate of flow, $q_0 = dV/dt$, can be related to the pressure drop, Δp; the number of capillaries per unit area, N; the filtration area, A; the diameter and length of capillaries, $2r_0$ and h; and the solution viscosity, μ_f, by the expression

$$q_0 = \frac{dV}{dt} = \frac{\pi NAr_0^4 g_c \Delta p_0}{8h\mu_f} \quad \text{(A4)}$$

and as the pores plug during filtration by

$$q = \frac{\pi NAr^4 g_c \Delta p}{8h\mu_f} \quad \text{(A5)}$$

provided that the flow through the packing voids of the layer of retained solids on the pore walls is negligible compared to flow

through the main channel of the pore. Rearrangement gives

$$r_0^2 = \left(\frac{q_0}{\pi N A g_c \Delta p_0}\right)^{0.5} \quad (A6)$$

$$r^2 = \left(\frac{q}{\pi N A g_c \Delta p}\right)^{0.5} \quad (A7)$$

Substitution of values from (A6) and (A7) in (A3) gives

$$\pi N A h\left[\left(\frac{q_0}{\pi N A g_c \Delta p_0}\right)^{0.5} - \left(\frac{q}{\pi N A g_c \Delta p}\right)^{0.5}\right] = \frac{cV}{1-\epsilon_p} \quad (A8)$$

or

$$\left(\frac{q_0/(g_c\Delta p_0)}{8\pi N A h^3 \mu_f}\right)^{0.5} - \left(\frac{q/(g_c\Delta p)}{8\pi N A h^3 \mu_f}\right)^{0.5} = \frac{cV}{1-\epsilon_p} \quad (A9)$$

setting

$$\left(\frac{g_c}{8\pi N A h^3 \mu_f}\right)^{0.5} = \beta \quad (A10)$$

Then

$$\left(\frac{q_0}{\Delta p_0}\right)^{0.5} - \left(\frac{q}{\Delta p}\right)^{0.5} = \left(\frac{c}{1-\epsilon_p}\right)\beta V \quad (A11)$$

which is the general differential form of the standard-blocking law.

For constant-pressure operation Equation (A11) becomes

$$\left(\frac{q_0}{\Delta p_0}\right)^{0.5} - \left(\frac{q}{\Delta p_0}\right)^{0.5} = \left(\frac{c}{1-\epsilon_p}\right)\beta V \quad (A12)$$

Rearranging gives

$$q = \frac{dV}{dt} = \Delta p_0\left[\left(\frac{q_0}{\Delta p_0}\right)^{0.5} - \frac{\beta c V}{(1-\epsilon_p)}\right]^2 \quad (A13)$$

Integrating gives

$$\int_0^V \frac{dV}{\left[\left(\frac{q_0}{\Delta p_0}\right)^{0.5} - \frac{\beta c V}{1-\epsilon_p}\right]^2} = \Delta p_0 \int_0^t dt \quad (A14)$$

$$\frac{V}{\left(\frac{q_0}{\Delta p_0}\right)^{0.5}\left[\left(\frac{q_0}{\Delta p_0}\right)^{0.5} - \frac{\beta c V}{(1-\epsilon_p)}\right]} = \Delta p_0 t \quad (A15)$$

Rearrangement of Equation (A15) yields the form

$$\frac{V}{t} = q_0 - \left(\frac{\beta c}{1-\epsilon_p}\right)(q_0^{0.5}\Delta p^{0.5})V \quad (A16)$$

or by further rearrangement, the form

$$\frac{t}{V} = \frac{1}{q_0} + \left(\frac{\beta c}{1-\epsilon_p}\right)\left(\frac{\Delta p_0}{q_0}\right)^{0.5} t \quad (A17)$$

where the K_s of the Hermans and Bredée equation equals

$$\left(\frac{2\beta c}{1-\epsilon_p}\right)\left(\frac{\Delta p_0}{q_0}\right)^{0.5}$$

Equation (A17) can be made more understandable and significant in terms of filter-medium behavior if the terms Δp_0, β, and q_0 are replaced by terms containing the filter-medium constants. This can be done by substituting Equations (A5) and (A10) in (A17) to give

$$\frac{t}{V} = \frac{8h\mu_f}{\pi N A r_0^4 g_c \Delta p} + \left(\frac{g_c}{\pi N A h^3 \mu_f}\right)^{0.5} \cdot \left(\frac{h\mu_f}{\pi N A r_0^4 g_c}\right)^{0.5}\left(\frac{c}{1-\epsilon_p}\right)t \quad (A18)$$

or, simplified,

$$\frac{t}{V} = \left(\frac{8h}{\pi N r_0^4}\right)\left(\frac{\mu_f}{A g_c \Delta p}\right) + \left(\frac{c/(1-\epsilon_p)}{\pi N A h r_0^2}\right)t \quad (A19)$$

This shows that the slope of a t/V vs. t plot during the period of standard blocking (the $K_s/2$ of Hermans and Bredée's equation) is equal to the packed volume of solids removed per volume of filtrate divided by the effective pore volume of the area of filter medium used. Thus, with $c = c_f$, the volume of solids per unit volume solution in the feed suspension, assumed and the probable value of ϵ_p known from independent measurements on the particulate solids, the clogging value of the medium, $\pi N h r_0^2$, can be solved for directly from the slope of the t/V vs. t plot over the standard-blocking region. The pore-resistance constant, $8h/\pi N r_0^4$, can also be calculated from the extrapolated intercept of the standard-blocking region. Solution for individual terms N, h, and r_0 is not possible by use of these values alone. If the filter medium were truly composed of straight-through circular pores of uniform radius, the relationship $N = \epsilon/\pi r_0^2$ becomes valid and a direct solution for values of N, h, and r_0 would become possible. However, since the actual pores of the filter medium are of nonuniform cross section along their length, the major areas of plugging are probably restricted to the constrictions within these pores. Although these constrictions will not all be at the same depth within the filter medium, it seems reasonable that under these conditions this plugging area or minimum free area will be less than ϵA and can be written as $a\epsilon A$, where a is the fractional free cross-sectional area represented by the pore constrictions which actually plug. For an actual filter medium, the population density of the pores can then be written as

$$N = \frac{a\epsilon}{\pi r_0^2} \quad (A20)$$

where r_0 is the radius of the pore constrictions which plug and a is the fractional free cross-sectional area represented by pore constrictions of this radius. This leads to four unknown terms, N, a, h, and r_0, and direct solution with the three independent relationships available is not possible. However, measurement of any one will allow calculation of the remainder. Measurement of pore-size distribution by the mercury-intrusion technique actually reflects the distribution of pore constriction and thereby offers a means of measuring one of these variables, thus permitting calculation of the remainder.

This same procedure can be applied to relate the characteristics of the filter medium to performance over the standard-blocking region for the case of constant-rate filtration. For constant-rate filtration $q = q_0$ and the general differential form of the standard-blocking equation [Equation (A11)] can be written as

$$\frac{1}{\Delta p^{0.5}} = \frac{1}{\Delta p_0^{0.5}} - \left(\frac{\beta}{q_0^{0.5}}\right)\left(\frac{c}{1-\epsilon_p}\right)V \quad (A21)$$

Substituting the values of β and q_0 given by Equations (A5) and (A10) gives

$$\frac{1}{\Delta p^{0.5}} = \frac{1}{\Delta p_0^{0.5}} - \left(\frac{g_c}{8\pi N A h^3 \mu_f}\right)^{0.5} \cdot \left(\frac{8h\mu_f}{\pi N A r_0^4 g_c \Delta p_0}\right)^{0.5}\left(\frac{cV}{1-\epsilon_p}\right) \quad (A22)$$

Simplifying and rearranging gives

$$\left(\frac{\Delta p_0}{\Delta p}\right)^{0.5} = 1 - \left(\frac{c/(1-\epsilon_p)}{\pi N A h r_0^2}\right)V \quad (A23)$$

Thus the slope of a plot of $(\Delta p_0/\Delta p)^{0.5}$ vs. V should allow direct calculation of the clogging value, $\pi N h r_0^2$, for the filter medium during constant-rate filtration. However, direct solution for N, a, h, and r_0 is again not possible if all are unknown.

Inspection of Equation (A19) for constant-pressure filtration shows that neither Δp nor μ_f should have any direct effect on the slope of the t/V vs. t plot during the period of standard blocking, but that both affect the intercept directly. However, changes in Δp can be expected to have considerable indirect effect by changing the values of c_f, ϵ_p, and r_0. The r_0 term of the clogging value will decrease with increasing Δp because of compression of the medium. Values of c_f and ϵ_p can be expected to decrease with increasing Δp because of the increasing shear stress, $r(\Delta p)/2h$, in the pores. If direct interception is the controlling mechanism of particle retention, changes in μ_f should have no effect on constant-pressure filtrations provided that the same Δp is used and shear stress within the pores is similar from run to run.

Similar consideration of Equation (A22) for a constant-rate filtration shows that changes in rate of filtration or the viscosity have no direct effect on the slope of the $(\Delta p_0/\Delta p)^{0.5}$ vs. V plots of such data. However, changes in either q_0 or μ_f can be expected to have a large indirect effect by changing the values of r_0, c_f, and ϵ_p. Thus, if either q_0 or μ_f is left constant and the other increased, the value of Δp_0 increases, causing increased initial compression of the medium and an increased shear stress, $(\mu_f/g_c)(4q/\pi r^3)$, in the pores at any point in the filtration cycle.

Presented at A.I.Ch.E. New York meeting